Aus der Medizinischen Klinik mit Schwerpunkt Hepatologie und
Gastroenterologie, Campus Virchow Klinikum,
der Medizinischen Fakultät Charité – Universitätsmedizin Berlin

DISSERTATION

The effect of omega-3 fatty acids on hepatocellular carcinoma in a transgenic mouse model

zur Erlangung des akademischen Grades
Doctor medicinae (Dr. med.)

vorgelegt der Medizinischen Fakultät
Charité – Universitätsmedizin Berlin

von

Lena Friederike Olgun

aus Berlin

Datum der Promotion: 10.03.2017

DIRECTORY

Figures

Tables

Abbreviations used

5-HETE	5-hydroxyeicosatetraenoic acid
8-HETE	8-hydroxyeicosatetraenoic acid
15-HETE	15-hydroxyeicosatetraenoic acid
17-HDHA	17-hydroxyeicosahexaenoic acid
18-HEPE	18-hydroxyeicosapentaenoic acid
AA	arachidonic acid
ALT	alanine aminotransferase
AST	aspartate aminotransferase
ATL	aspirin-triggered lipoxins
CCl_4	carbon tetrachloride
COX	cyclooxygenase
DAPI	4', 6-diamino-2-phenylindole dihydrochloride
DEN	diethylnitrosamine
DHA	docosahexaenoic acid
DOB	date of birth
DT	docosatrienes
EGF	epidermal growth factor
EPA	eicosapentaenoic acid
EET	epoxyeicosatrienoic acids
H&E	hematoxylin and eosin stain
HBV	hepatitis B virus
HCC	hepatocellular carcinoma
HCV	hepatitis C virus
IL	interleukin
IGF	insulin growth factor
JNK	c-Jun N-terminal kinase
LC-MS/MS	liquid chromatography tandem mass spectrometry analysis

LPS	lipopolysaccharide
LT	leukotriene
MAPK/ERK	mitogen activating protein kinase and extracellular signal-regulated kinase
min.	minutes
MRI	magnetic resonance imaging
mRNA	messenger ribonucleic acid
n-3-PUFA	omega-3 polyunsaturated fatty acids
n-6-PUFA	omega-6 polyunsaturated fatty acids
NASH	non-alcoholic steatohepatitis
NFκB	nuclear factor kappa-light-chain-enhancer of activated B-cells
ns	not significant
PBS	phosphate buffered saline
PD1	protectin D1
PDGF	platelet derived growth factor
PG	prostaglandin
ROS	reactive oxygen species
RvD_{1-6}	resolvin D_{1-6}
RvE_1	resolvin E_1
SMA	smooth muscle actin
TGF-α	transforming growth factor alpha
TLR	Toll-like receptor
TNF-α	tumor necrosis factor alpha
TXA	thromboxane
VEGF	vascular endothelial growth factor
wt	wild type

1 Abstract

1.1 Abstract

Liver tumors, particularly hepatocellular carcinoma (HCC), are a major cause of morbidity and mortality worldwide. The development of HCC is mostly associated with chronic inflammatory liver disease of various etiologies. Previous studies have shown that omega-3 (n-3) polyunsaturated fatty acids (PUFA) dampen inflammation in the liver and decrease formation of TNF-α. The study presented here aimed to investigate the influence of an increased tissue status of n-3 PUFA on hepatocellular carcinogenesis.

We used the transgenic fat-1 mouse model, which endogenously forms n-3 PUFA from n-6 PUFA, to determine the effect of an increased n-3 PUFA tissue status on tumor formation in the diethylnitrosamine (DEN)-induced liver tumor model. At 8 months of age, we examined the 15 livers (9 fat-1 and 6 wild-type mice in the control group) by MRI, macroscopically and microscopically, measured markers of inflammation in the serum and evaluated inflammation, fibrosis, and tumor formation using immunohistochemistry. We determined expression of NFκB, levels of PUFA and lipid mediators of liver tissue.

Our results showed a decrease in tumor formation, in terms of size and number of tumors in fat-1 mice compared to wild-type (wt) littermates, as documented by both in vivo measurements by MRI and in post-mortem gross assessments. The decreased tumorigenesis was associated with decreased plasma TNF-α levels in fat-1 mice, indicating decreased pro-inflammatory activity in these mice. Furthermore, there was less COX-2 expression and a decreased activation of hepatic stellate cells in the livers of fat-1 mice reflecting a lower fibrotic activity. Lipidomics analyses of lipid mediators revealed significantly increased levels of the n-3 PUFA-derived 18-hydroxyeicosapentaenoic acid (18-HEPE) and 17-hydroxydocosahexaenoic acid (17-HDHA) in the livers of fat-1 animals treated with DEN, which could contribute to the dampened inflammation status in these animals.

The results of this study provide evidence that an increased tissue status of omega-3 polyunsaturated fatty acids suppresses liver tumorigenesis, likely through inhibiting liver inflammation. The findings also point to a potential anti-cancer role for the n-3 PUFA-derived lipid mediators 18-HEPE and 17-HDHA, which down-regulate the important pro-inflammatory and pro-proliferative factor TNF-α.

1.2 Zusammenfassung

Tumorerkrankungen der Leber, insbesondere das hepatozelluläre Karzinom (HCC), gehen weltweit mit hohen Morbiditäts- und Mortalitätsraten einher. Chronisch entzündliche Lebererkrankungen unterschiedlicher Ätiologie bilden die Hauptursache der Entstehung von HCC. Es ist bekannt, dass omega-3 (n-3) mehrfach ungesättigte Fettsäuren (PUFA) sowohl die Entzündungsreaktion in der Leber als auch die Bildung des Tumornekrosefaktoralphas (TNF-α) vermindern. Ziel dieser Forschungsarbeit war es, den Einfluss von einer erhöhten n-3 PUFA-Konzentration im Lebergewebe auf die hepatozelluläre Karzinogenese zu untersuchen.

Um den Effekt eines erhöhten n-3 PUFA Gehalts auf die Tumorentstehung in einem Diethylnitrosamin (DEN)-induzierten Tumormodel messen zu können, verwendeten wir das transgene fat-1 Mausmodel, welches n-6 PUFA endogen zu n-3 PUFA umwandelt. Im Alter von 8 Monaten erfolgte bei den insgesamt 15 Mäusen (9 fat-1 und 6 Wildtyp-Mäuse in der Kontrollgruppe) die mikroskopische und makroskopische Untersuchung der Mäuselebern, welche durch Magnetresonanztomographie (MRT) ergänzt wurde, die Messung der serologischen Entzündungsparameter sowie eine immunhistochemische Analyse der Tumorentwicklung und des Entzündungs- und Fibrosierungsgrads der Leber. Darüber hinaus wurden die Expression von NFκB sowie die PUFA- und Lipidmediatorenspiegel im Lebergewebe bestimmt.

Die in-vivo MRT-Messungen wie auch die post-mortem durchgeführten makroskopischen Untersuchungen der Mäuse ergaben, dass die fat-1 Mäuse im Vergleich zu ihren Geschwistern vom Wildtyp hinsichtlich der Tumorgröße und -anzahl eine deutlich verminderte Tumorentwicklung aufwiesen. Diese ging mit verminderten TNF-α-Plasmaspiegeln, einer geringeren Expression von COX-2 und einer reduzierten Aktivierung von hepatischen Ito-Zellen einher, was auf eine abgemilderte pro-inflammatorische und fibrotische Aktivität hinweist. Die Analyse der Lipidmediatoren ergab zudem signifikant erhöhte Spiegel der von n-3 PUFA abgeleiteten 18-Hydroxyeicosapentaensäure (18-HEPE) und 17-Hydroxydocosahexaensäure (17-HDHA) im Lebergewebe der DEN-behandelten fat-1 Mäuse, was zum verminderten Entzündungsgrad beigetragen haben könnte.

Die Ergebnisse unserer Untersuchungen liefern klare Hinweise darauf, dass eine erhöhte Konzentration von omega-3 mehrfach ungesättigten Fettsäuren im Lebergewebe von Mäusen die Entwicklung hepatischer Tumore unterdrücken kann. Der

Mechanismus dahinter scheint über eine Hemmung der begleitenden hepatischen Entzündungsreaktion vermittelt zu werden. Diese Resultate deuten auf eine potentiell anti-maligne Eigenschaft der von n-3 PUFA abstammenden Lipidmediatoren 18-HEPE und 17-HDHA hin, welche den pro-inflammatorischen und pro-proliferativen Faktor TNF-α down-regulieren.

2 Introduction

2.1 Hepatocellular carcinoma

Liver tumors are a big clinical problem in humans. Primary liver cancer is the fifth most common cancer worldwide and the third most common cause of cancer mortality (1). 85% to 90% of all primary liver cancers are hepatocellular carcinomas (HCC) (2). HCC arises only rarely in the healthy liver but usually in chronically inflamed tissue. The risk of hepatocarcinogenesis increases vastly at the cirrhosis stage (2). It is now recognized that inflammation in the tumor microenvironment is a hallmark of cancer and that cancer-associated inflammation stimulates tumor progression (3, 4). Thus, treatment of chronic inflammatory liver diseases is a possible approach to prevention of HCC.

2.1.1 Epidemiology

The distribution of liver cancer incidence varies throughout the world. Over 80% of HCC cases occur in sub-Saharan Africa and Eastern Asia. Particularly China has a very high incidence rate: it accounts for more than 50% of the world's cases (age-standardized incidence rate: men, 35.2/100,000; women, 13.3/100,000) (2). In the United States, HCC is the quickest increasing cause of cancer-related death in men (5). In Germany, the incidence rate of HCC is 5-10/100,000.

HCC incidence also varies between different ethnic groups living in the same region. To give an example, HCC rates in the United States are the highest among Asians, second in African Americans, and lowest in whites. A possible explanation for this ethnic variability might include differences in the prevalence and acquisition time of main risk factors for liver disease and HCC (2).

In most populations the incidence rates of HCC are higher in males than in females, with male/female ratios between 2:1 and 4:1 (2). There are different approaches to explain the higher rates of liver cancer in males. Firstly, they may relate to gender specific differences in exposure to risk factors. Men are more frequently infected with HBV and HCV and are also more likely to drink alcohol and to smoke cigarettes. However, even in mouse experiments it was shown that male mice were two- to eight-times more prone to develop HCC in comparison with female mice (6). These results support the assumption that androgens contribute to enhance HCC progression rather

than sex-specific exposure to risk factors. Interestingly, several studies from Taiwan described a positive correlation between increased circulating testosterone levels and HCC in HBV-infected men (7, 8).

2.1.2 Etiology

The most important risk factors for hepatocellular carcinoma vary by region. In most high-rate countries, the leading risk factor is chronic HBV infection. The other major HCC risk factor in high-risk areas is the consumption of aflatoxin B_1-contaminated food. The increasing quantity of people living with cirrhosis is a probable explanation for the rising frequency of HCC in low-rate HCC areas (2).

HCC primarily occurs in chronically inflamed liver tissue in the context of cirrhosis (~70% - 90% of all detected HCC cases). Cirrhosis in patients with HCC is most often caused by hepatitis B, hepatitis C, alcoholic liver disease, and sometimes by non-alcoholic steatohepatitis. Less commonly it is caused by autoimmune hepatitis, α-1 antitrypsin deficiency, hereditary hemochromatosis, and some porphyrias (2).

In comparison to the general population, case-control studies demonstrated that chronic HBV carriers are 5- to 15-fold more likely to develop HCC (2).

Despite being a major risk factor for the formation of HCC, the risk of developing HCC among chronically HCV-infected persons is not easy to assess because only few adequate long-term cohort studies exist; it probably lies between 1% and 3% after 30 years (9). HCV increases HCC risk by advancing fibrosis and ultimately cirrhosis. Once HCV-related cirrhosis has occurred, HCC develops with the likelihood of 1% to 4% each year (2). 15% to 35% of HCV-infected patients develop liver cirrhosis 25-30 years after infection (10).

Another well-known HCC risk factor is heavy alcohol intake (over 50-70 g/day for prolonged periods). Heavy alcohol intake leads to the development of cirrhosis, but there is little evidence of a direct carcinogenic effect (2). Furthermore, heavy alcohol ingestion exhibits a synergistic effect with HBV/HCV infection and increases the risk of developing HCC, likely by more actively promoting cirrhosis (11).

Animal studies have confirmed that aflatoxin B_1 is a powerful hepatocarcinogen. It is a mycotoxin produced by the Aspergillus fungus, that readily grows on foodstuffs like corn and peanuts stored in warm and damp conditions (12).

A study by El-Serag et al. implied that diabetes mellitus is a moderately strong risk factor for HCC (13).
Experimental studies have established a link between inflammation and hepatocellular carcinogenesis and have found an important role of TNF-α in tumor development (14-17). TNF-α promotes liver cell proliferation in the context of chronic inflammation, leading to enhanced tumorigenesis in the liver.

2.1.3 Diagnostic imaging

Imaging is very important for diagnosing and staging hepatocellular carcinoma.
Multiple studies reported that the validity of ultrasound and its results strongly depend on the experience of the examiner, the technology used, the body habitus, the presence of cirrhosis, and the size of the tumor (18, 19). Latest studies indicated a >60% sensitivity, and >90% specificity (20). When it comes to identifying tumor nodules in cirrhotic livers, the sensitivity of ultrasound is especially low (19, 21, 22).
Choi et al. stated in 2001 that the most reliable diagnostic tests are triple-phase helical computed tomography (CT) and triple-phase dynamic contrast enhanced magnetic resonance imaging (MRI) (23). There have been several studies that compared the accuracy of CT and MRI for HCC diagnosis, providing evidence that MRI is slightly better in the characterization and diagnosis of HCC in comparison with CT scans (24-26). A systematic review and meta-analysis performed by Lee et al. in 2015 showed that MRI had higher per-lesion sensitivity than multidetector CT and should be the preferred imaging modality for the diagnosis of HCCs in patients with chronic liver disease (27).

2.1.4 Current therapeutic approaches

Prevention of HCC can be achieved by treatment of chronic inflammatory liver diseases, while treatment of this tumor entity is mainly limited to surgical or local-ablative procedures, and chemotherapy is not yet routinely administered in the treatment of HCC.
One of the most commonly used staging systems is the BCLC (Barcelona Clinic Liver Center) classification which is based on the evolutionary course of tumor progression and liver disease and which allows for prediction of life expectancy and choice of treatment modality for patients (28). Accordingly, potentially curative treatments for

patients with *early stages* of HCC development (1 HCC or 3 nodules < 3 cm) include hepatic resection, orthotopic liver transplantation and percutaneous ablation methods like radio frequency ablation and percutaneous ethanol injection. The tumor location, degree of portal hypertension, severity of decrease in liver function and presence of medical comorbidities mainly dictate the selection of therapy.

In the group of patients in the *intermediate stage* (multinodular but without portal vein thrombosis), with compensated cirrhosis and without HCC-related symptoms or vascular invasion, transarterial chemoembolization leads to an improvement in survival compared with conservative therapy.

Sorafenib, an oral multikinase inhibitor, is a palliative treatment option for patients who are considered as being at an *advanced stage* (metastases, portal invasion), with mild cancer-related symptoms and/or vascular invasion or extrahepatic spread.

The 1-year survival rate of patients who fall into the *terminal stage* category is less than 10% (18).

Chemotherapies are currently not routinely administered in the treatment of HCC, but are mainly targeted at different points along tyrosine kinase receptor pathways, including vascular endothelial growth factor (VEGF), platelet derived growth factor (PDGF), epidermal growth factor (EGF), and insulin growth factor (IGF). Tyrosine kinase receptors are related to HCC progression when they activate the intracellular MAPK/ERK signaling pathway by activating Ras. Bevacizumab is a recombinant humanized antibody against VEGF and Brivanib is a dual inhibitor of VEGF receptor and fibroblast growth factor receptor pathways. Sorafenib is the first drug shown to improve survival of patients, and is a humanized monoclonal antibody and an oral multi-kinase inhibitor of VEGF, PDGF, EGF and IGF, which interferes with the cascade to induce angiogenesis and vascularization (28).

Prognosis is limited, and most patients eventually succumb to the disease. In population-based studies in the United States, the overall 1- and 3- year survival rates for patients diagnosed with HCC were found to be 20 % and 5 %, respectively (29).

2.2 Experimental hepatocellular carcinoma

2.2.1 HCC animal models

Rodents are often used for cancer research for various reasons: humans and rodents have multiple physiologic and genetic similarities, rodents have a short lifespan and can be bred easily (30).

There are several different mouse models for the study of HCC: chemically induced models, xenograft models and genetically modified models.

Chemically induced HCC mouse models mimic the injury-fibrosis-malignancy cycle by administration of a genotoxic compound like N-nitrosodiethylamine (DEN), peroxisome proliferators, aflatoxin B_1, Carbon tetrachloride (CCl_4), a choline deficient diet or thioacetamide (30).

In xenograft models, hepatoma cell lines are implanted either ectopically or orthotopically in mice. This method is suitable for drug screening, but results can only be extrapolated if multiple cell lines are used. The hollow fiber method is a solution to limit the number of test animals used in xenograft research as multiple different cell lines may be implanted in one mouse (30).

Moreover, mice have been genetically modified to explore the pathophysiological and molecular features of HCC (31). Transgenic mice express viral genes, oncogenes and/or growth factors used to investigate pathways involved in hepatocarcinogenesis (30).

2.2.2 DEN-induced HCC

Chemically induced HCC are the preferred models for HCC research, as they mimic the injury-fibrosis-malignancy cycle seen in humans (30).

DEN's carcinogenic capacity is due to its ability to alkylate DNA structures. In the first step, DEN is hydroxylated to α-hydroxyl nitrosamine (32). This bioactivation step is oxygen- and NADPH-dependent and is mediated by cytochrome P450, an enzyme that has its highest activity in the centrilobular hepatocytes. After cleavage of acetaldehyde, an electrophilic ethyldiazonium ion is formed. This ethyldiazonium ion causes DNA damage by reacting with nucleophiles such as DNA-bases. Additionally, oxidative stress caused by DEN can contribute to hepatocarcinogenesis (33). Reactive oxygen species (ROS) are known to cause DNA, protein and lipid damage by forming hydrogen

peroxide and superoxide anions generated by the P450-dependent enzymatic system (34, 35).

HCC develops after a single postnatal injection of DEN in mice (15, 16). If used in older mice, a tumor promoter like phenobarbital is necessary to induce carcinogenesis (30). The time needed for the development of HCC after a single DEN-injection is determined not only by the age, but also by the administered dose, the sex, and strain of mice (36). Younger mice have higher hepatocyte proliferation rates and thus HCC is induced faster in juvenile as compared to adult animals (37). The gender-related difference is attributed to the inhibitory effect of estrogens and the stimulating effect of androgens on hepatocarcinogenesis (38). Genetically, the DEN-model establishes an appropriate representation of HCC associated with poor prognosis (39).

2.3 Polyunsaturated fatty acids and lipid mediators

A fatty acid is a carboxylic acid with a long unbranched aliphatic tail (chain) at one end and a methyl group at the other. They can be classified according to the length of the acyl-chain, its functional groups, the number of double bonds and the position of the first double bond. Fatty acids are classified by the number of double bonds into saturated, monounsaturated and polyunsaturated fatty acids (Fig. 2.3). Saturated fatty acids are long-chain carboxylic acids that have no double bonds, monounsaturated fatty acids are fatty acids that have one double bond in the fatty acid chain and all of the remainder of the carbon atoms in the chain are single-bonded. Polyunsaturated fatty acids contain at least two carbon-carbon double bonds. Fatty acid viscosity and melting temperature increases with decreasing number of double bonds. Physiologically, the double bonds of polyunsaturated fatty acids in the human body are in cis-configuration.

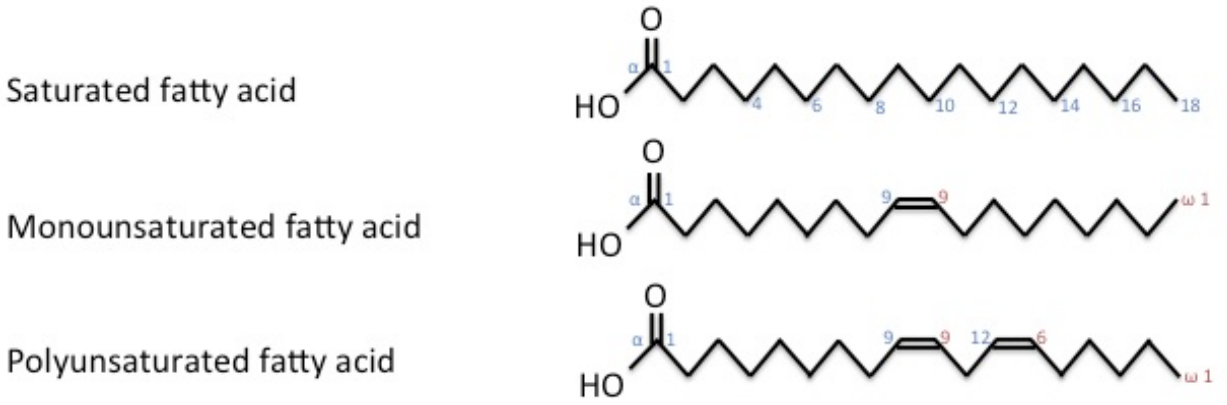

Figure 2.3. *Fatty acid overview: example of a saturated fatty acid, stearic acid (18:0), a monounsaturated fatty acid, oleic acid (18:1, n-9), and a polyunsaturated fatty acid, linoleic acid (18:2, n-6).*

2.3.1 Omega-3 and omega-6 PUFA

Omega-3 and omega-6 fatty acids belong to the group of unsaturated fatty acids. Omega (ω) is the last letter in the Greek alphabet and marks the last carbon atom of the fatty acid chain furthest away from the carboxy group (COOH). Omega-3 implies that the last double bond in the polyunsaturated carbon chain of the fatty acid is located in the third C-C bond from the methyl end of the fatty acid ("omega minus 3"). Likewise, omega-6 fatty acids have a double bond six carbons away from the methyl carbon end (Fig. 2.3.1).

Essential fatty acids are molecules that cannot be synthesized de novo by humans and other mammals but are vital for biological processes. Two essential fatty acids are known for humans: α-linolenic acid (18:3, n-3; ALA) and linoleic acid (18:2, n-6; LA). Mammals lack the enzymes to introduce double bonds at carbon atoms beyond C-9 in the fatty acid chain. The human body has limited ability to form the "long-chain" n-3 fatty acids eicosapentaenoic acid (20-carbon atoms) and docosahexaenoic acid (22-carbon atoms) from the "short-chain" 18-carbon omega-3 fatty acid α-linolenic acid (ALA) (40, 41).

Omega-3 and omega-6 should be consumed in a balanced proportion and researchers consider a ratio of n-6:n-3 in the range of 1:1 to 1:4 as healthy (42). Studies suggest that the evolutionary human diet, rich in seafood, nuts and other sources of omega-3

fatty acids, may have provided such a ratio (43). Nowadays, typical Western diets provide ratios of between 10:1 and 30:1 (44). Considering the crucial role of n-3 PUFA-derived lipid mediators, this imbalance in diet could be of great importance in the pathology of many so-called civilization diseases (42).

The main dietary sources are canola oil for ALA and cold water oily fish such as salmon, herring, mackerel, anchovies and sardines for EPA and DHA. Although fish is a dietary source of omega-3 fatty acids for humans, fish cannot synthesize them themselves. Algae are the primary producers of DHA and EPA in the ecosystem and fish receive their high n-3 fatty acid levels from the algae they consume (41).

The n-6 polyunsaturated fatty acid (PUFA) linoleic acid is mainly found in palm, soybean, rapeseed, and sunflower oils. Arachidonic acid (20:4, n-6; AA) is a PUFA that is present in the phospholipids of animal cell membranes and is largely being consumed with animal fats, meats and egg yolks.

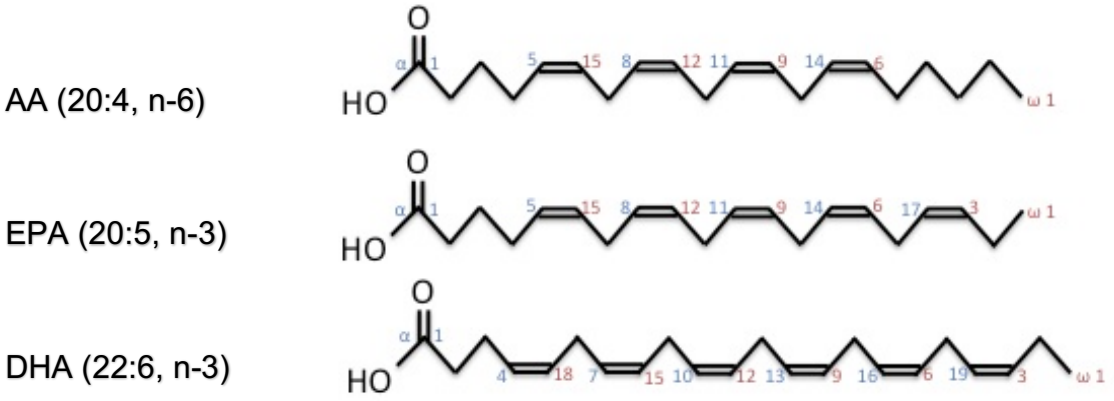

Figure 2.3.1. *Examples of n-3 and n-6 PUFAs: arachidonic acid (AA, top), eicosapentaenoic acid (EPA, middle), and docosahexaenoic acid (DHA, bottom).*

2.3.2 Lipid mediators

Polyunsaturated fatty acids (PUFA) such as the omega-6 PUFA arachidonic acid (AA) and the omega-3 PUFAs eicosapentaenoic acid (EPA) and docosahexaenoic acid (DHA) play an important role in inflammation and proliferation by functioning as

precursors of highly potent pro- and anti-inflammatory mediators (45) (Fig. 2.3.2). Eicosanoids (*eicosa* is Greek for “20”) are a diverse family of metabolites derived from the 20-carbon fatty acid AA, including prostaglandins, thromboxanes, leukotrienes, and lipoxins (46). Arachidonic acid is the origin of many chiefly pro-inflammatory mediators, such as prostaglandins (PG), thromboxanes (TX) and leukotrienes (LT). These lipid mediators are formed by enzymatic action of enzymes such as cyclooxygenases (COX) and lipoxygenases (LOX). Most cells express COX-1 constitutively as a housekeeping enzyme. Inflammatory stimuli induce expression of the closely related enzyme COX-2, they generate the prostanoids (46). Nonsteroidal anti-inflammatory drugs (NSAIDS) inhibit COX which catalyzes an early step in the pathway from arachidonate to prostaglandins and thromboxanes (47). Macrophages and white blood cells produce 5-lipoxygenase (5-LO) which synthesizes leukotrienes and lipoxins. Leukotrienes mediate inflammatory reactions by constricting smooth muscle in the respiratory tract and constricting blood vessels, allowing plasma to leak from small vessels (LTC_4) and attracting white blood cells into connective tissue (LTB_4) (46).

The subscript indicates the number of double bonds: The EPA-derived prostanoids have three double bonds, (e.g. PGG_3, PGH_3, PGI_3, TXA_3) while its leukotrienes have five, (LTB_5). The AA-derived prostanoids have two double bonds, (e.g. PGG_2, PGH_2, PGI_2, TXA_2) while its leukotrienes have four, (LTB_4).

Prostaglandins have an array of functions, e.g. elevating body temperature (producing fever) and causing inflammation and pain. Thromboxanes are produced by platelets and act in the formation of blood clots and the reduction of blood flow to the site of a clot (47).

Epoxyeicosatrienoic acids (EETs) are signaling molecules formed by the action of cytochrome P450 epoxygenase on AA. They modulate ion transport and gene expression, producing vasorelaxation as well as anti-inflammatory and pro-fibrinolytic effects. A number of fatty acid epoxide derivatives are produced directly from EETs by COX, CYP ω-oxidase or glutathione *S*-transferase. Others are formed by rearrangements of 12- or 15-hydroperoxyeicosatetraenoic acid (HPETE), the lipoxygenase products formed from arachidonic acid by 12- and 15-lipoxygenase, respectively (48).

Lipoxins comprise a series of anti-inflammatory mediators. Their appearance in inflammation signals the resolution of inflammation. Lipoxins are high-affinity antagonists to the cysteinyl leukotriene receptor 1 (CysLT1) to which several

leukotrienes (LTC_4, LTD_4, LTE_4) mediate their smooth muscle contraction and eosinophil chemotactic effects.

EPA and DHA function as precursors of the anti-inflammatory resolvins (Rv) and protectins. Resolvins derived from EPA are termed resolvins of the E-series (RvE), and resolvins derived from DHA are termed RvD. Resolvins and protectins are potent stereoselective agonists that control the duration and magnitude of inflammation. In addition to their origins in inflammation resolution, these compounds also display potent protective roles in neural systems, liver, lung, and eye. The actions of resolvins include reducing neutrophil traffic, regulating cytokine and reactive oxygen species, and lowering the magnitude of the response. Protectins demonstrate anti-inflammatory and neuroprotective actions in vivo (49).

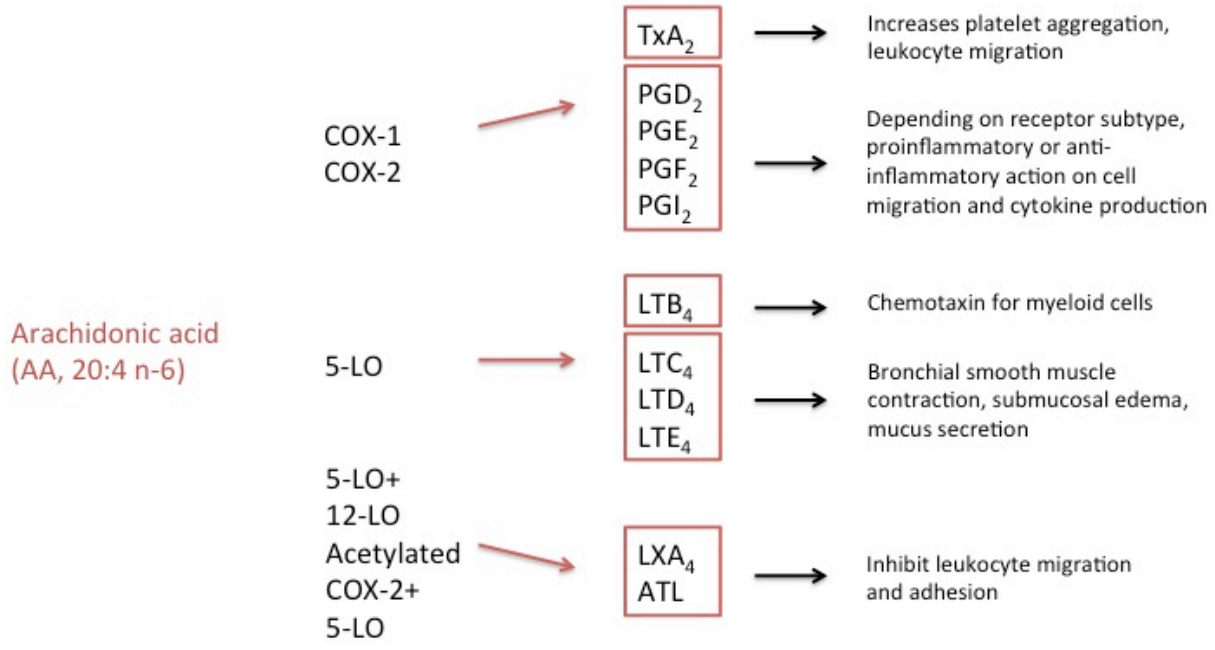

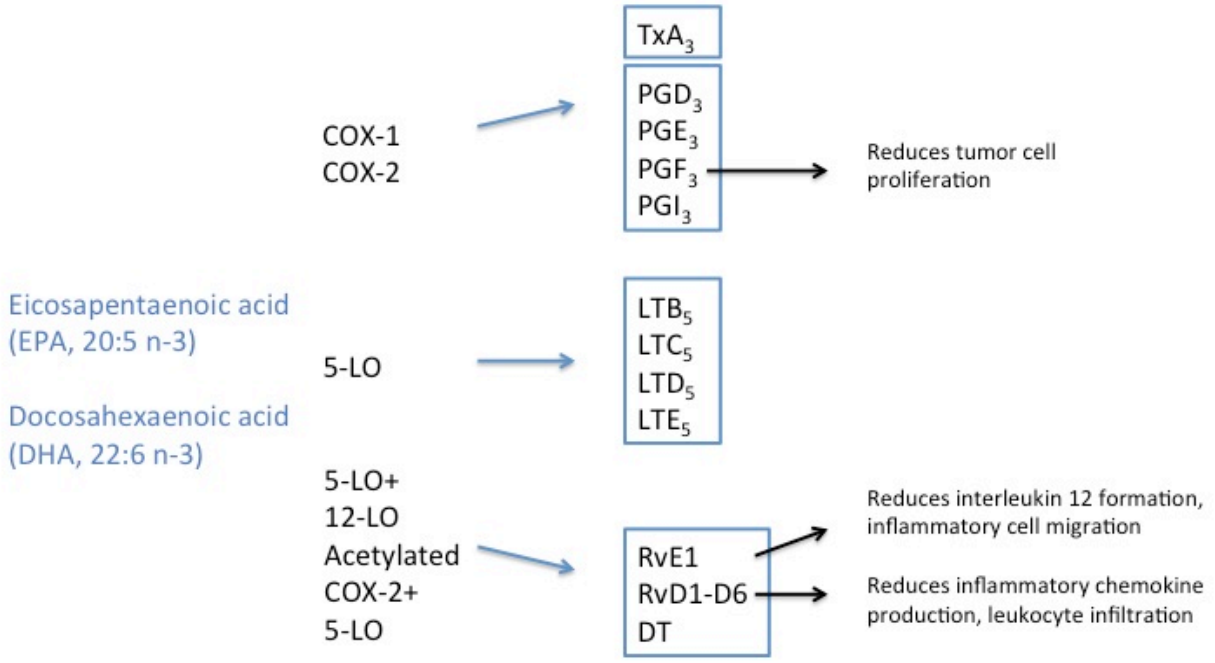

Figure 2.3.2. *n-6 and n-3 PUFA and some of their metabolites and biological effects (45).*

2.3.3 Resolvins and protectins

A new series of lipid mediators generated from n-3 essential fatty acids has been identified by lipidomic analyses in exudates that were collected during the resolution phase of acute inflammatory response in mice (50-52). During the resolution phase of acute inflammatory response, cell-cell interactions and transcellular biosynthesis lead to production of novel bioactive lipid mediators from DHA and EPA, termed resolvins (resolution phase interaction products) and protectin D1 (50-52). EPA is a precursor of Resolvin E1 (RvE1), a new bioactive oxygenated product that was recently identified and characterized (53). Resolvin E1 was found to inhibit nuclear factor κB (NFκB) activation and production of cytokines through binding to the specific ChemR23 receptor (53, 54). Protectin D1, a bioactive DHA product generated from the metabolic intermediate 17*S*-hydro(peroxy)-DHA potently regulates critical events associated with inflammation and its resolution (Fig. 2.3.3), including inhibition of polymorphonuclear cells (PMN) infiltration and T cell migration and reduction of tumor necrosis factor α (TNF-α) and Interferon-γ (IFNγ) secretion, chemokine formation, and interleukin 1 (IL-1)-induced NFκB activation (55-58).

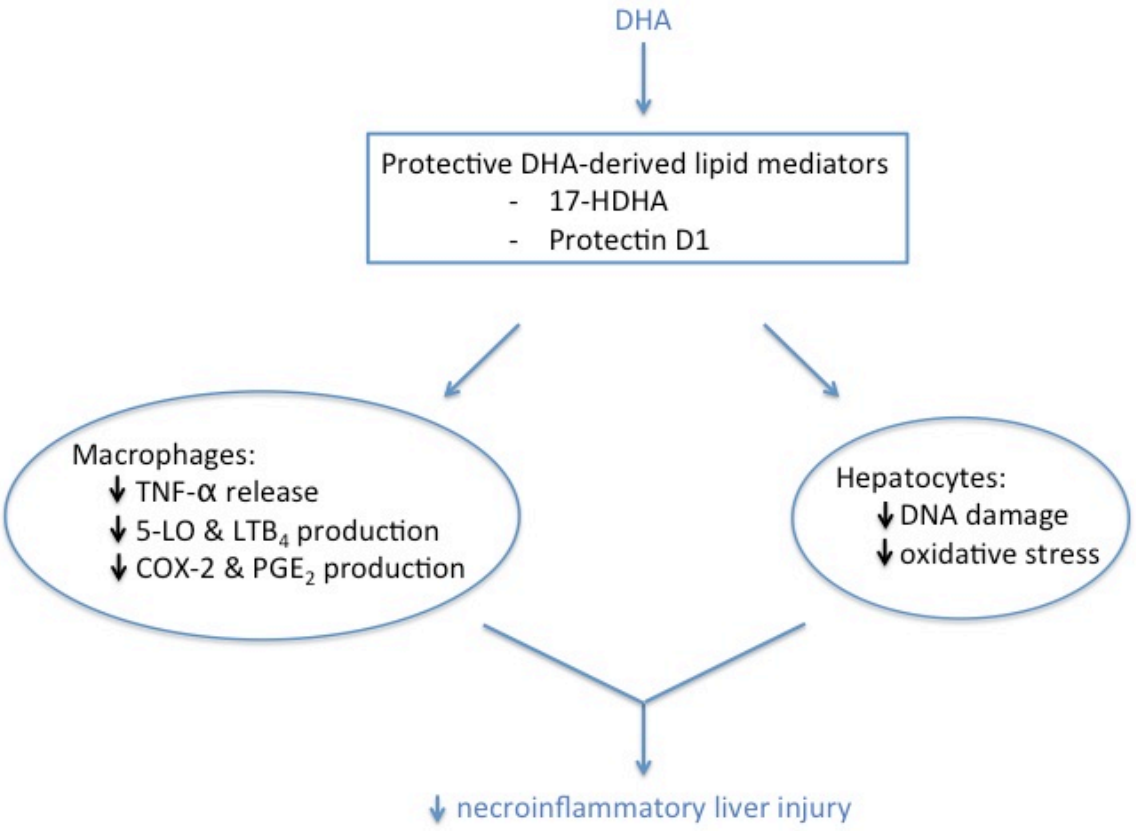

Figure 2.3.3. *Formation and protective actions of DHA-derived lipid mediators in the liver.* Protectin D1 and 17S-HDHA may ameliorate necroinflammatory liver injury by down-regulating TNF-α release and 5-LO and COX-2 activities in macrophages and by reducing DNA damage and oxidative stress in hepatocytes (59).

2.3.4 Anti-inflammatory effects of omega-3

Numerous in vitro, animal and clinical experiments suggest diverse biologically relevant effects of omega-3 (n-3) fatty acids, including immunoregulatory, anti-thrombotic and anti-inflammatory as well as anti-tumor and anti-metastatic action. Long-chain n-3 essential fatty acids have frequently been reported to have effects contrary to those of AA and to display potent anti-inflammatory properties. Dietary interventions rich in DHA and/or EPA have been shown to dampen inflammation and are used as preventive measures against illnesses such as rheumatoid arthritis, cystic fibrosis, ulcerative colitis, asthma, atherosclerosis, cancer, and cardiovascular disease (60). In a recent study in

the laboratory of Prof. Jing X. Kang, the transgenic *fat-1* mouse was used to analyze the effect of an increased n-3 PUFA tissue status in the macrophage-dependent acute D-galactosamine/ lipopolysaccharide (D-GalN/LPS) hepatitis model (61). These results were similar to the inflammation dampening observed in the fat-1 mouse model with dextrane sodium sulfate (DSS)-induced colitis (62).
Several theories have been discussed to explain how dietary n-3 fatty acids counter the inflammatory effects of AA's eicosanoids: displacement, competitive inhibition and direct counteraction. Dietary n-3 fatty acid intake decreases the tissue concentrations of AA, partly because ALA displaces LA from the elongase and desaturase enzymes that produce AA. Also, EPA inhibits phospholipase A_2's release of AA from cell membranes. Competition of EPA and DHA with AA for metabolisation by cyclooxygenases and lipoxygenases results in diminished amounts of AA-derived mediators such as prostaglandins (PG), thromboxane of the 2-series and leukotrienes (LT) of the 4-series and formation of less potent n-3 derived mediators (63).
Some EPA derived eicosanoids counteract their AA-derived counterparts, e.g. EPA yields the antiaggregatory prostacyclin PGI_3 and also the leukotriene LTB_5 which vitiates the action of the AA derived LTB_4.

Recent studies have analyzed lipidomic aspects in the context of non-alcoholic steatohepatitis (NASH) pathology (64, 65), demonstrating an increase in the ratio of n-6 to n-3 PUFA in NASH liver tissue as well as in the plasma levels of the AA metabolites 5-HETE, 8-HETE and 15-HETE in the progression from normal to NASH. These data indicate that the liver is critical not only for lipoprotein and triglyceride metabolism, but also for the conversion of essential PUFAs to bioactive lipid mediators, due to the expression of COX, LOX and cytochrome P450 enzymes. The n-6/n-3 PUFA ratio in liver tissue probably determines the lipid mediator profile generated and could thus be an important factor in the development of liver disease.

However, the molecular mechanisms underlying the beneficial actions of n-3 essential fatty acids remain to be clearly identified.

2.3.5 A transgenic approach

Since mammals cannot naturally produce n-3 fatty acids from the more abundant n-6 fatty acids, they rely on a dietary supply. In order to analyze the effect of an increased omega-3 PUFA tissue status but at the same time ruling out the possible confounding factors of diverging diets (e.g. content of trace elements, fibers, antioxidants) (66), we used the transgenic fat-1 mouse in this study.

The transgenic fat-1 mouse was generated on a C57BL/6 background in the laboratory of Prof. Jing X. Kang at Massachusetts General Hospital (67). The fat-1 transgenic mice express a desaturase from the roundworm Caenorhabditis elegans that enables them to add a double bond into an unsaturated fatty-acid hydrocarbon chain and thus to endogenously form n-3 PUFA from corresponding n-6 PUFA. This means that not only the n-3 proportion of the organism's fatty acid profile rises, but that the n-6 proportion decreases as well. This results in a stronger shift of the n-6/n-3 ratio (67).

Given the diverse anti-inflammatory and anti-carcinogenic actions of n-3 derived lipid mediators, we assumed they could also play an important role in HCC development.

2.4 The role of pro-inflammatory cytokines in HCC

2.4.1 TNF-α

Experimental studies have established a link between inflammation and hepatocellular carcinogenesis and have found an important role for TNF-α in tumor development (14, 16, 17, 68).

Several studies have implicated n-3 PUFA in the dampening of inflammation in the liver by a TNF-α–dependent mechanism (59, 61): In a previous study in fat-1 mice with a balanced n-6/n-3 PUFA tissue content, decreased inflammatory liver injury was seen after induction of acute hepatitis by DGal-LPS, which results from activation of Kupffer cells. The study demonstrated lower inflammatory cytokine expression (TNF-α, IL-1β, IFN-γ and IL-6) in these animals, and this was associated with a decreased rate of apoptosis in livers from fat-1 animals as compared to wildtype (wt) mice (61).

Another study demonstrated that DHA supplementation led to increased formation of DHA-derived lipid mediators such as 17-HDHA and protectin D1 (PD1), which were able to protect the liver from CCl_4-induced necroinflammatory damage (59). This study also

showed that the protective effect was associated with decreased hepatic cyclooxygenase-2 (COX-2) expression and that 17-HDHA can suppress TNF-α-secretion from cultured murine macrophages. TNF-α promotes liver cell proliferation in the context of chronic inflammation, leading to enhanced tumorigenesis in the liver.

2.4.2 COX-2

Cyclooxygenase (COX) is a key enzyme in the biosynthesis of prostaglandins, thromboxanes and other eicosanoids from arachidonic acid. COX-1 is constitutively expressed and active in most cells; COX-2 is only present in some cells, like leukocytes and macrophages, and is there mostly inducible by endotoxins, cytokines and growth factors. It plays an important role in the development of fever, inflammation and pain.
Gonzalez-Periz et al. monitored changes in the pro-inflammatory COX-2 pathway in mice fed DHA-enriched diets which led to significant decreases in hepatic COX-2 mRNA expression and prostaglandin (PG) E_2 levels (59).

2.4.3 NFκB

In its inactive state, NFκB is bound to its inhibitor IκB in the cytoplasm. Several agonists, such as IL-1, IL-18, TNF-α and TLR ligands, activate NFκB (69). It is activated in cholestasis, autoimmune liver diseases and hepatitis B and C, which are linked with the development of HCC (70). The anti-inflammatory effect seen in colitis models with increased tissue levels of n-3 PUFA and with resolvin E1 treatment seems to be mediated, at least in part, by inhibition of the activity of the pivotal pro-inflammatory transcription factor NFκB (53, 54, 62).
Quite in contrast to results in colon carcinogenesis (71), it was shown that in chemically induced HCC inhibition of NFκB activity in hepatocytes increased cancer development. Inactivation of the IKKβ gene in hepatocytes resulted in higher HCC rates as well as in bigger size of the tumors (16). Deletion of IKKβ in hepatocytes led to increased proapoptotic c-Jun N-terminal kinase (JNK) -activity, in turn promoting TNF-α-induced cell death. Cell death in the liver is then followed by an extensive compensatory proliferation of hepatocytes, which is critical for tumor promotion, causing initiated hepatocytes to enter the cell cycle and transmit oncogenic mutations to their progeny (72). This leads eventually to carcinogenesis and higher rates of HCC development.

3 Research goals

3.1 Formulation of the problem

n-3 PUFA have been widely implicated in the dampening of inflammation and carcinogenesis (73), but the mechanism by which this occurs is unknown. In order to further clarify the role of omega-3 PUFA in carcinogenesis, we conducted a study on hepatocellular carcinoma in transgenic fat-1 mice.

Fat-1 mice can endogenously synthesize n-3 PUFA from n-6 PUFA without using dietary supplementation (67), thereby eliminating potential confounding factors of diet (66). These mice were recently used in a genetic hepatoma model in mice containing mutations in c-myc and TGF-α (transforming growth factor-alpha) (74), as well as in an inoculation liver tumor model (75). Both models demonstrated significant anti-tumor activity in the fat-1 mice. However, both studies focused primarily on protein analysis, notably demonstrating lower NFκB and COX-2 expression in the fat-1 livers, respectively. Analysis of n-3 PUFA lipid metabolites was not performed so far.

3.2 Objectives

We therefore decided to investigate the influence of an increased tissue status of n-3 PUFA and decreased n-6/n-3 PUFA ratio on HCC carcinogenesis. Hence, we induced HCC by treatment with diethylnitrosamine (DEN) in fat-1 mice and in wild type mice (control group). DEN is metabolized into an alkylating agent that induces DNA damage and mutations as well as hepatocyte death, leading to subsequent proliferation and regeneration dependent on cytokines (15). Important sources of these factors are Kupffer cells, which produce TNF-α and IL-6 in an IKKβ-dependent manner (16).

Based on the results obtained by Maeda et al. and Sakurai et al., and on the previous results in fat-1 mice studying macrophage-dependent acute hepatitis, we hypothesized a suppression of DEN-induced hepatocellular carcinogenesis in the fat-1 mouse due to a decreased inflammatory response associated with increased tissue status of n-3 PUFA and presence of n-3 PUFA-derived lipid mediators (15, 16).

In order to compare defined parameters of tumor development such as tumor number and tumor size, we used Magnetic Resonance Imaging (MRI) and microscopic analyses, analyzed fatty acid content and lipid mediator concentrations and conducted analyses

of relevant pro- and anti-inflammatory parameters in the livers and in the serum of treated animals.

3.3 Questions

1) Are fat-1 mice protected from HCC?
2) Are differences in size and number of the tumors discernible?
3) How do omega-3 fatty acids interfere in HCC development caused by DEN?
4) Will the histological evaluation of fat-1 mouse livers differ from wt livers concerning grading, staging and degree of inflammation?
5) As representative measures of inflammation, liver injury and tumorigenesis, another question of interest for us was in what way certain parameters would be different in the two experimental groups (e.g. neovascularization, hepatic cell damage, COX-2 expression, NFκB expression, Kupffer cell invasion, stellate cell activity or pro-inflammatory cytokine TNF-α levels).

4 Materials and Methods

4.1 Animals

4.1.1 The fat-1 transgenic mouse model

We used the transgenic fat-1 mouse, expressing a Caenorhabditis elegans desaturase, which endogenously forms n-3 PUFA from n-6 PUFA (67). Mice were crossed back at least four times onto C57BL/6, a widely used inbred mouse strain that possesses a high degree of genetic and phenotypic uniformity. To obtain wt and transgenic mice from the same offspring, generations of heterozygous fat-1 mice and wt mice were mated. The mice were phenotyped according to the n-6/n-3 PUFA ratio in their tails determined by gas chromatography (76). All experiments were conducted with fat-1 heterozygous male mice because female mice are less sensitive to DEN-induced carcinogenesis due to hormonal factors (77, 78).

4.1.2 Animal housing

The mice were fed ad libitum with an identical diet rich in omega-6 fatty acids (n-6 PUFA) and low in n-3 fatty acids (modification of TestDiet® AIN-76A Semi-Purified Diet 58B0 with 10% Total Corn Oil). Mice were maintained in a specific pathogen-free, air-conditioned environment in filter-topped cages with a controlled light cycle of 12 hours and received autoclaved food and water at the animal facility of Massachusetts General Hospital in Boston according to National Institutes of Health guidelines. All studies were approved by the Massachusetts General Hospital Subcommittee on Research Animal Care.

4.1.3 Sacrifice

Mice were sacrificed eight months after their date of birth (DOB) using a pentobarbital anesthesia to conduct cardiocentesis to increase the blood yield for further investigation. Blood samples were filled into sterile, heparinized tubes, centrifuged to obtain pure serum, frozen in liquid nitrogen and stored at -80°C. Livers were removed, separated into individual lobes and analyzed for the presence of HCCs. Liver lobes and other

organs were then fixed in formalin or frozen in liquid nitrogen and stored at -80°C until used for further analysis.

4.2 Tumor induction and experimental setup

4.2.1 Tumor induction and analysis

Fifteen-day-old male mice (approximate weight 7-8 g) were injected intraperitoneally (ip.) with 5 mg/kg Diethylnitrosamine (DEN) (Sigma). DEN is metabolized into an alkylating agent that induces DNA damage and mutations as well as hepatocyte death (68). Hepatocyte proliferation then ensues in response to DEN exposure and is dependent on cytokine growth factors and Kupffer cells. Hepatocellular carcinoma develops after a single postnatal injection of DEN in mice.

After 8 months mice underwent an MRI-Scanning of their livers, which enabled us to compare the exact tumor volume, regarding not just the number, but also the size of each tumor nodule. Afterwards all mice were sacrificed and their livers removed, separated into individual lobes and stored at -80°C (Table 4.2.1).

Table 4.2.1. *Experimental setup of groups (DEN-induced HCC).*

Group	Treatment	Age at sacrifice	Number of animals	MRI
Fat-1	DEN 5 mg/kg	8 months	9	at the time of sacrifice
wt	DEN 5 mg/kg	8 months	6	at the time of sacrifice

4.3 Tumor measurements and evaluation

4.3.1 Magnetic resonance imaging (MRI)

Small animal MR imaging is a non-invasive method for assessing and comparing tumor mass in the living animal. MRI was performed and read by Dr. Xiangzhi Zhou and Dr.

Yanping Sun of the Brigham and Women's Hospital, Boston. The mice need not be sacrificed to enumerate the tumor nodules and could be counted only once (at the day of sacrifice), instead, they can be followed up in the development of tumor growth. Until now only few research groups have used this method, thus we wanted to rate the tumor numbers and sizes determined by MRI compared to the conventional method of counting the externally visible tumors exceeding 0.5 mm.

Mice were scanned at eight months after DOB and sacrificed on the next day. Measurements were carried out using a 4.7T Bruker Avance horizontal bore system equipped with a 200-mm inner diameter gradient set capable of 30 G/cm gradient strength. To reduce motion artifacts in this procedure all mice were anesthetized with 1.5-2% isoflurane in an oxygen/air mixture via nose cone during the *in vivo* MR scan.

A T1 weighted spin echo sequence with TR = 450ms, TE = 6.41ms, was used throughout the entire study. For axial scan, the slice thickness was 1mm and the number of slices was sufficient to cover the entire liver so that a measurement of the tumor volume was possible. The matrix size is 128 ´ 128 and FOV is 3.50 ´ 3.50 cm^2. The respiration of the mice was monitored and adjusted at a rate of 20-40 breaths per minute. The scan time for axial imaging was about 8 minutes with NEX = 8. All animals were scanned using identical settings and parameters as described above. Tumor mass identification and calculations were done by an experienced radiologist and compared to the macroscopic findings in the sacrificed animals afterwards. For tumor volume measurement in the livers, the area of each tumor in the different slices was manually marked and then these areas were multiplied by the slice thickness. Single tumor volumes then resulted from adding these individual volumes from consecutive slices. Total tumor volume per liver was calculated by adding the different tumor volumes.

4.3.2 Measurements of externally visible tumors

To evaluate the effect of n-3 PUFA, we first quantified the extent of HCC-induction. Externally visible tumors (≥ 0.5 mm) were counted and measured by stereomicroscopy immediately after sacrificing the animals. Lobes were then separated, fixed in formalin or frozen in liquid nitrogen and stored at -80°C until used for further analysis.

4.3.3 Histological tumor evaluation

To quantify the morphologic changes of HCC development, histological examination was performed in a blinded manner. Grading, staging and the degree of inflammation were assessed by an experienced pathologist. Liver tissue samples for histological examination were fixed in 10% neutral buffered formalin (37% formaldehyde 100 ml, monobasic sodium phosphate 4 g, dibasic sodium phosphate 6.5 g and 900 ml distilled water), embedded in paraffin, sectioned into 7-µm-thick slices and samples of each mouse were stained with hematoxylin and eosin (H&E), trichrome and reticulin stain, respectively.

4.3.3.1 Hematoxylin and eosin stain

The paraffin embedded tissue sections were first deparaffinized in M-Xylene (CAS-number 108-38-3, Fluka, Sigma-Aldrich), rehydrated from 100% ethanol to PBS, and then stained with hematoxylin for 2 min (Gill 2 formulation; Ricca Chemical Company), rinsed in tap water, dipped in eosin (Eosin yellowish solution 1% w/v; Fisher Scientific, SE23-500D), rinsed in deionized water and finally dehydrated again to 100% ethanol.
Since the lungs are the most common site for HCC metastases we also investigated H&E stained lung tissue slides to assess possible metastases in fat-1-lungs compared to wt mice.

4.3.3.2 Reticulin stain

The reticulin stain following the Gordon and Sweet's method is a silver impregnation technique that demonstrates reticular fibers. The reticular fibers in a normal liver are well-defined strands, but necrotic and cirrhotic livers show discontinuous patterns and tumorous tissue forms characteristic patterns of thickened reticular fibers. The technician in the pathologist's laboratory performed the reticulin stain.
In short, the principle of this stain is that the tissue is first oxidized (1% acidified potassium permanganate for 2 min., rinsed in distilled water and bleached in 1% oxalic acid solution) and then sensitized with 2.5% iron alum for 10 minutes, which is replaced with silver solution (at 4°C for 20 seconds) and washed well in several changes of distilled water. The silver is reduced with 10% aqueous formalin solution to its visible metallic state. Slides are then treated with 5% sodium thiosulphate for 5 min., rinsed in

tap water and counterstained in eosin for 1 minute. In the end, reticular fibers appear to be black and the nuclei red.

4.3.3.3 Trichrome stain

Lillie's Trichrome Stain is a routine stain for liver biopsies used to differentiate between collagen and smooth muscle in tumors, and the increase of collagen in diseases such as cirrhosis. For this stain, three dyes are employed, selectively staining muscle (red), cytoplasm (Biebrich Scarlet - light red/pink), collagen fibers (Aniline Blue - blue) and nuclei (Weigert's hematoxylin - dark brown/black). The general rule in trichrome staining is that the less porous tissues are colored by the smallest dye molecule and whenever a dye of a larger molecular size is able to penetrate it will always do so at the expense of the smaller molecule. The trichrome stain was performed by the technician in the pathologist's laboratory.

The slides were deparaffinized and rehydrated through 100%, 95% and 70% alcohol and washed in distilled water. To improve staining quality, sections were re-fixed in Bouin's solution (picric acid, formaldehyde and glacial acetic acid) for 1 hour at 56°C and rinsed in running tap water. The sections were then stained in Weigert's iron hematoxylin solution (hematoxylin, alcohol, 29% ferric chloride in water, distilled water and concentrated hydrochloric acid) for 10 minutes, washed in distilled water and stained in Biebrich scarlet-acid fuchsin solution for 10-15 minutes and then rinsed again. Differentiation was achieved through staining in phosphomolybdic-phosphotungstic acid solution for 10-15 minutes and then stained in aniline blue solution for 5-10 minutes. After differentiation in 1% acetic acid solution for 2-5 minutes, the sections were dehydrated in ethyl alcohol and xylene. In addition to the scoring system used by our pathologist, the connective tissue content was evaluated by comparing the area stained with blue dye in the liver tissue of fat-1 mice to the dyed area in liver tissue of wt mice.

4.3.3.4 Scoring System

Our scoring system consisted of the following items:

I) In liver tissue the grade of inflammation was evaluated by rating

- **necrosis** (0 = absent, 1 = spotty necrosis, one or few necrotic hepatocytes, 2 =

multifocal necrosis, 3 = bridging necrosis, 4 = confluent necrosis)

- **fibrosis** (0 = absent, normal lobular architecture, 1 = pericentral fibrosis, increased thickness of the central vein, 2 = central anastomoses, some fibrous septa connecting central veins, 3 = precirrhotic stage, fibrous septa with marked distortion of the liver lobules, 4 = cirrhosis, nodule regeneration surrounded by broad connective tissue septa)
- **steatosis** (percentage of tissue area, 0 = 0%, 1 = < 33%, 2 = < 66%, 3 = > 66%)

II) Tumors of liver tissue were evaluated concerning

- **number of foci** of HCC
- **size** of detected tumors in mm
- **differentiation state** (1 = well, 2 = moderately, 3 = poorly differentiated)
- **lymphovascular invasion** (0 = absent, 1 = present)

4.4 Immunohistochemistry

Visualization of an antibody-antigen interaction can be accomplished with immunohistochemistry to understand the distribution and localization of differentially expressed proteins in biological tissues. Its principle is based on the binding of an antibody to its specific antigen. Usually, an antibody is conjugated to an enzyme, such as peroxidase, that can catalyze a color-producing reaction. Alternatively, the antibody can also be tagged to a fluorescent dye (e.g. fluorescein or Alexa Fluor), which can be detected in a highly sensitive manner by confocal laser microscopy.

For COX-2, CD31 and F4/80 staining, liver tissue was fresh-frozen in Tissue-Tek® OCT medium (Ted Pella Inc., Redding, CA, USA), and sections were cut at 5 µm thickness. After air-drying, the unspecific protein binding sites were blocked with normal goat serum (Lampire Biological Laboratories, Pipersville, PA). Sections were then incubated overnight at room temperature in a moist chamber with the primary antibodies mentioned below, rinsed with PBS/Tween (Gibco 10010 pH 7.4 1x, Invitrogen; Fisher Scientific Tween 20 enzyme grade BP337-500) and incubated with secondary antibodies in the same manner. All secondary antibodies were used in a 1:200 dilution. Sections were mounted with Glycergel mounting medium (Dako, Cambridgeshire, UK) and evaluated with a LSM 5 Pascal confocal microscope (Carl Zeiss AG, Oberkochen,

Germany).

4.4.1 α-smooth muscle actin (α-SMA) stain

Fresh liver tissue was fixed in 10% neutral buffered formalin overnight, followed by automated processing and embedding in paraffin. For α-SMA staining, the slides were exposed to a 1:25 diluted anti-α-SMA antibody (Thermo-Fischer-Scientific) for 10 min at room temperature. After washing with PBS, the primary anti-α-SMA antibody was detected using an Alexa fluor 595 antibody (1:1000 dilution). Stainings were quantified by counting the number of α-SMA-positive cells in 3 high power fields (HPF) per mouse by two different blinded observers, positive cells located in or near blood vessel walls were ignored, and the mean value of these counts was used for further analysis. Data are expressed as the number of α-SMA-positive cells per HPF. For visualization of liver cell nuclei, cells were co-stained with DAPI (4',6-diamino-2-phenylindole dihydrochloride) in an aqueous dilution of 1:10.000 for 2 min.

4.4.2 Cyclooxygenase-2 (COX- 2) stain

For COX-2 determination, fresh frozen sections were incubated over-night with an anti-murine COX-2 antibody (1:50 dilution; Cayman), followed by staining with a horseradish peroxidase (HRP) conjugated secondary antibody (goat anti-rabbit in 5% normal goat serum; KPL Inc., Gaithersburg, MD, USA) detected by 3,3'-diaminobenzidine-substrate (DAB) and counterstained with hematoxylin. COX-2 positive cells were counted for quantification when showing a brownish cytoplasmatic staining and analysis was made comparing the percentage of positively stained areas.

4.4.3 Staining of endothelial cells (CD31 positive) in tumor tissue

To determine intratumoral microvascular density, cryopreserved tumor sections were immunostained with an affinity-purified anti-mouse CD31 (PECAM-1) antibody generated in rat (1:100 dilution; eBioscience) and incubated with the fluorescein isothiocyanate (FITC) labeled goat anti-rat IgG secondary antibody. Sections were counterstained with DAPI.

4.4.4 Staining of macrophages (F4/80 positive)

The affinity-purified anti-mouse F4/80 Antigen - Pan Macrophage Marker, BM8 (eBioscience) monoclonal antibody generated in rat reacts with mouse F4/80 antigen. The F4/80 antigen is expressed by a majority of mature macrophages and other cell types such as Langerhans cells and liver Kupffer cells.
Cryopreserved sections of liver tissue were immunostained with the above-named antibody (1:100 dilution) and subsequently incubated with the FITC-labeled goat anti-rat IgG secondary antibody. Sections were counterstained with DAPI.

4.5 ALT- and AST-levels in serum

The enzymes alanine transaminase (ALT) and aspartate transaminase (AST) are located in very high concentrations in the cytoplasm of hepatocytes and only in low concentrations in other tissues. In case of hepatic cell damage, ALT and AST are released into circulation, where they accumulate and their activity can be measured.
Thus, liver injury was also examined by the quantitative determination of the circulating transaminases' ALT and AST enzyme activity in serum using the ALT- and AST-detection kits from Biotron Diagnostics Inc. (Hermet California, USA). The Biotron Diagnostics method is a modification of the Reitman and Frankel method (79). The enzyme alanine transaminase catalyzes an exchange of an amino group of alanine and aspartate, respectively, for a α-keto group of α-ketoglutarate. The end products formed in this reaction are pyruvate and glutamate and oxalacetate and glutamate, respectively, (the oxalacetate formed partially decomposes to pyruvate in a constant ratio under the conditions of the test). Dinitrophenylhydrazine was added to form the hydrazones of the pyruvate present. These hydrazones were reacted with sodium hydroxide to form a color that was read by a spectrophotometer (Shimadzu Scientific Instruments, Columbia, MD, USA) at a wavelength of 540 nm.

4.6 Tumor necrosis factor α levels in serum

To compare the levels of the pro-inflammatory cytokine TNF-α in serum, the Mouse TNF-α ELISA Ready-SET-Go! kit (eBioscience) was used following the manufacturer's protocols. First, the 96 well ELISA plate had to be coated overnight at 4°C with the

capture antibody diluted in coating buffer (purified anti-mouse TNF-α-antibody). After washing with Washing Buffer (1 x PBS, 0.05% Tween-20), wells were blocked with 1 x Assay Diluent (eBioscience, 5 x concentrated stock solution) for one hour at room temperature. To the prepared wells, 100 µl of serum of each mouse or the standard in different dilutions was added in duplicates. The TNF-α of the mouse sera and the standards bind to the antibodies during the overnight incubation at 4°C, forming strong antigen-antibody-bonds and will hence not be removed by the consecutive washing procedures that separate the steps. Afterwards, wells were first incubated with the polyclonal biotin-conjugated detection antibody (eBioscience) in 1 x Assay Diluent and then with the detection enzyme Avidin-HRP (eBioscience), each at room temperature for one hour. The colorimetric reaction was induced by adding the substrate solution (3,3',5,5'-Tetramethylbenzidine, 1 x solution), finished off with the stop solution (1 M H_3PO_4) and was measured in the luminometer at a wavelength of 450 nm.

4.7 NFκB-ELISA of liver tissue

The subunit p65 of NFκB was determined using an ELISA-based kit (EZ-Detect™ NFκB p65 Transcription Factor Kit, Pierce, Rockford, IL) and performed according to the manufacturer's instructions. The assay is based on the immunochemical detection of activated transcription factors in nuclear extracts using a subunit p65 specific antibody and an HRP-conjugated secondary antibody. Nuclear extracts from whole liver tissues were collected using the Nuclear Extraction Kit (Active Motif) and protein concentrations were determined by using a Coomassie Plus Assay (Coomassie Plus, Pierce, Rockford, IL).

4.7.1 Extraction of nuclear protein

50 mg of frozen liver tissue was crushed under liquid nitrogen using a cold mortar and pestle. The tissue powder was resuspended in 120 µl of a hypotonic buffer containing also DTT and detergent. After centrifugation at 850 x *g* for 5 min. at 4°C, the supernatant was discarded and the remaining pellet was resuspended in 100 µl of complete lysis buffer containing also DTT and a protease inhibitor cocktail. The cells were then gently dounced on ice with a dounce homogenizer (Fisher Scientific, Hampton, NH, USA) to aid in releasing the soluble nuclear fraction, incubated on ice for

30 min. to extract the nuclear proteins and centrifuged at 14,000 x *g* for 30 min. at 4°C to remove the insoluble material. Aliquots were diluted in lysis buffer and stored at -80°C until used.

4.7.2 Determination of protein concentrations

The Coomassie Plus Kit is a colorimetric method for total protein quantitation and is based on the Bradford assay for protein determination (80). When Coomassie dye binds protein in an acidic medium, an immediate shift in absorption maximum occurs from 465 nm to 595 nm with a concomitant color change from brown to blue. The formed complex can be read spectrometrically at a proportional relationship between absorption at 595 nm and protein concentration. Absolute values were determined by employing a standard curve with bovine serum albumin (BSA).

4.7.3 Performance of NFκB protein assay

Lysates (20 µg of nuclear extracts) were incubated at room temperature for one hour in a 96 well plate coated with NFκB consensus duplex. Consecutively, the primary antibody against p65 (dilution 1:1,000) and the horseradish peroxidase-conjugated secondary antibody (dilution 1:10,000) were incubated in the same manner, separated by washing steps. The reaction was developed with a chemiluminescent substrate (Luminol/Enhancer Solution) at room temperature and its intensity was measured immediately at 450 nm using a microplate reader (Victor 1420 Multilabel Counter, Wallac 1420 Workstation Software Version 3.00 Revision 2, Perkin Elmer, Wellesley, MA, USA).

4.8 Analysis of PUFA and lipid mediators

4.8.1 Gas chromatography

For phenotyping and fatty acid analysis, liver or mouse tail tissues frozen in liquid nitrogen were homogenized. An aliquot of tissue homogenate (<50 µl) was mixed in a glass methylation tube with 1.5 ml hexane and 1.5 ml Boron Tri-fluoride. After blanketing with nitrogen, the mixture was heated at 100°C for 1 hour, cooled to room temperature and methyl esters extracted in the hexane phase following addition of 1 ml

H_2O. The samples were centrifuged for 5 min., and then the upper hexane layer was removed and concentrated under nitrogen. Fatty acid methyl esters were analyzed by gas chromatography using a fully automated HP5890 system equipped with a flame-ionization detector (81). The chromatography utilizes an Omegawax 250 capillary column (30 m × 0.25 mm I.D.). Peaks were identified by comparison with fatty acid standards (Nu-chek-Prep, Elysian, MN), and area and its percentage for each resolved peak was analyzed using a Perkin-Elmer M1 integrator (76).

4.8.2 Lipid mediator analysis

Thirty milligrams of ground and frozen liver tissue was mixed with methanol and internal standard (consisting of absolute amounts of 10 ng LTB_4-d_4) and hydrolyzed with 300 µl of 10 M sodium hydroxide for 30 minutes at 60 °C. The solution was neutralized with 60% acetic acid and pH adjusted at 6.0 with sodium acetate buffer. A solid phase extraction was performed with anion exchange column (Bond Elute Certify II, Agilent, Santa Clara, CA) as previously described by Rivera (82). After centrifugation, the clear supernatant obtained was put on the preconditioned column. For elution of more hydrophilic metabolites like prostaglandins, thromboxanes and lipoxins we used an n-hexane : ethyl acetate extraction mixture of 25 : 75 with 1% acetic acid. The eluate was evaporated on a heating block at 40°C under a stream of nitrogen to obtain a solid residue. Residues were then dissolved in 70 µl acetonitrile. An Agilent 1200 HPLC system and a solvent system consisting of acetonitrile/0.1% formic acid in water was used. The gradient elution was started with 15% acetonitrile. This was increased within 10 minutes up to 90% and held for 10 minutes. The high-performance liquid chromatography was coupled with an Agilent 6410 Triplequad mass spectrometer with electrospray ionization source. Analysis of lipid mediators was performed using multiple reaction monitoring in negative mode.

4.9 Statistical analysis

Data were analyzed using Prism 3.02v Software (GraphPad, Inc.). Comparison was made using the Student's *t*-test or as indicated. All values are presented as the mean ± standard error of the mean (SEM) or as indicated. *P* values ≤ 0.05 were considered significant.

5 Results

5.1 Fatty acid profiles of liver tissues

Both wt and fat-1 transgenic littermates born to the same mother were maintained on a diet high in n-6 and low in n-3 PUFA. During this dietary regimen, fat-1 transgenic mice had significantly higher amounts of n-3 PUFA, such as EPA and DHA in all organs and tissues including the liver compared to wt mice. In order to quantify the major n-3 and n-6 PUFA and some of their metabolites, liver tissue from DEN-treated wt and fat-1 mice was analyzed using gas chromatography (Table 5.1). Results of gas chromatography showed that the content of EPA and DHA was significantly different between the two groups, with higher levels in the fat-1 mice. There were lower levels of AA in the liver tissue of fat-1 animals as compared with the wt mice, but this difference was not statistically significant. Fat-1 mice had a ratio of AA/(DHA + EPA) of 1.97 (n = 9) compared with a ratio of 9.06 in wt mice (n = 6).

Table 5.1. *PUFA profiles of livers from wt and fat-1 mice (mean ± SEM) showing higher levels of the n-3 PUFA EPA and DHA in fat-1 liver tissue.*

PUFA	wt (n = 6)	fat-1 (n = 9)	difference
n-6 (%)			
AA (20:4 n-6)	9.13 ± 1.20	8.52 ± 0.81	ns
n-3 (%)			
EPA (20:5 n-3)	0.00 ± 0.00	0.17 ± 0.02	p < 0.0001
DHA (22:6 n-3)	1.01 ± 0.26	4.15 ± 0.46	p < 0.001
total	1.01	4.32	
n-6/n-3 (of total fractions)	9.06	1.97	

5.2 Assessment of tumor incidence and tumor load

5.2.1 MRI analysis and quantification of tumor incidence and tumor load

The assessment of tumor load used to be restricted to superficially visible tumors on the surface of the livers of mice. It was impossible to judge the tumor load within the liver parenchyma from these measurements.

In order to assess tumor load inside the liver, we performed in vivo MRI-imaging before the mice were sacrificed. In the MRI scans performed here, T1-weighted images were sufficient to detect mouse liver tumors without application of contrast medium. In the T1-weighted protocol the tumors appeared either with higher or lower signal intensity than normal liver tissue (Fig. 5.2.1.1, 2, 3 and 4).

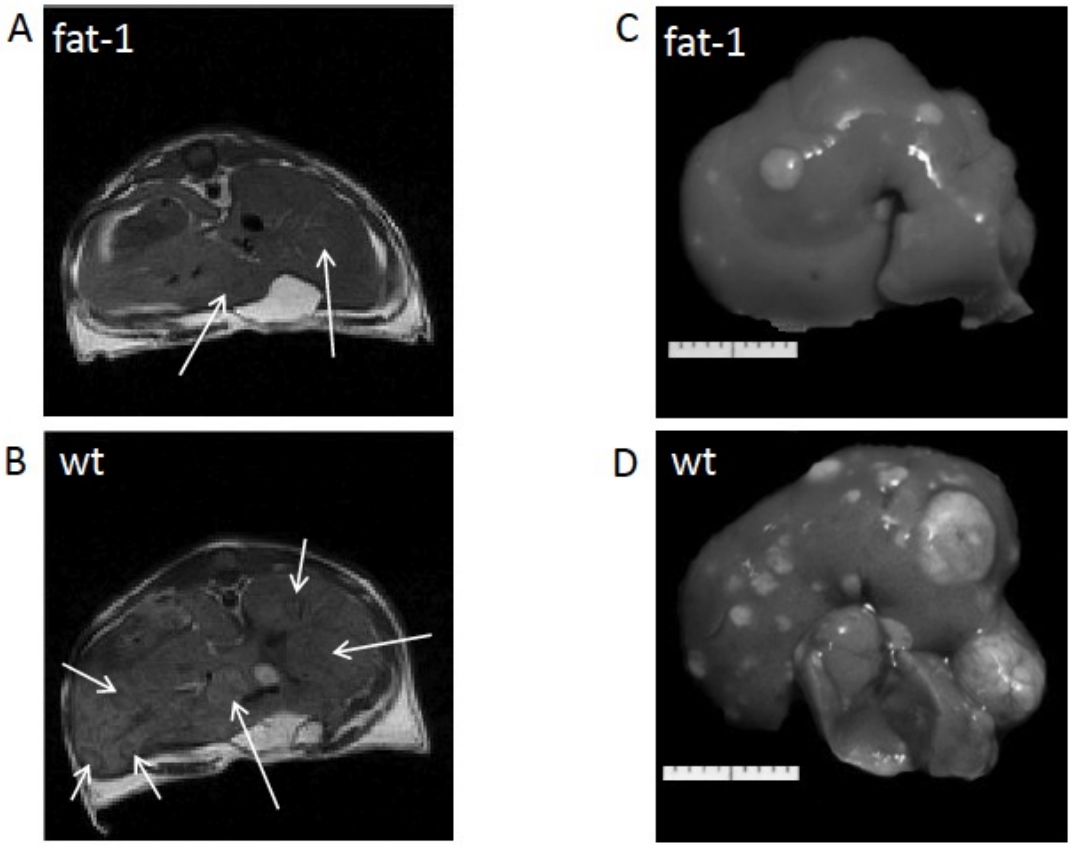

Figure 5.2.1.1. *Comparison of tumor load: MRI and gross photographs of wt and fat-1 mouse*

Total tumor volume per liver was significantly lower in fat-1 mice (Fig. 5.2.1.4). In several animals, there were large intraparenchymal tumors that could only be discerned by MRI and escaped the surface analysis of the organ. Representative examples of organs from fat-1 (Fig. 5.2.1.1C) and wt mice (Fig. 5.2.1.1D) are shown to demonstrate the differences in superficial tumor counts visible between the two groups.

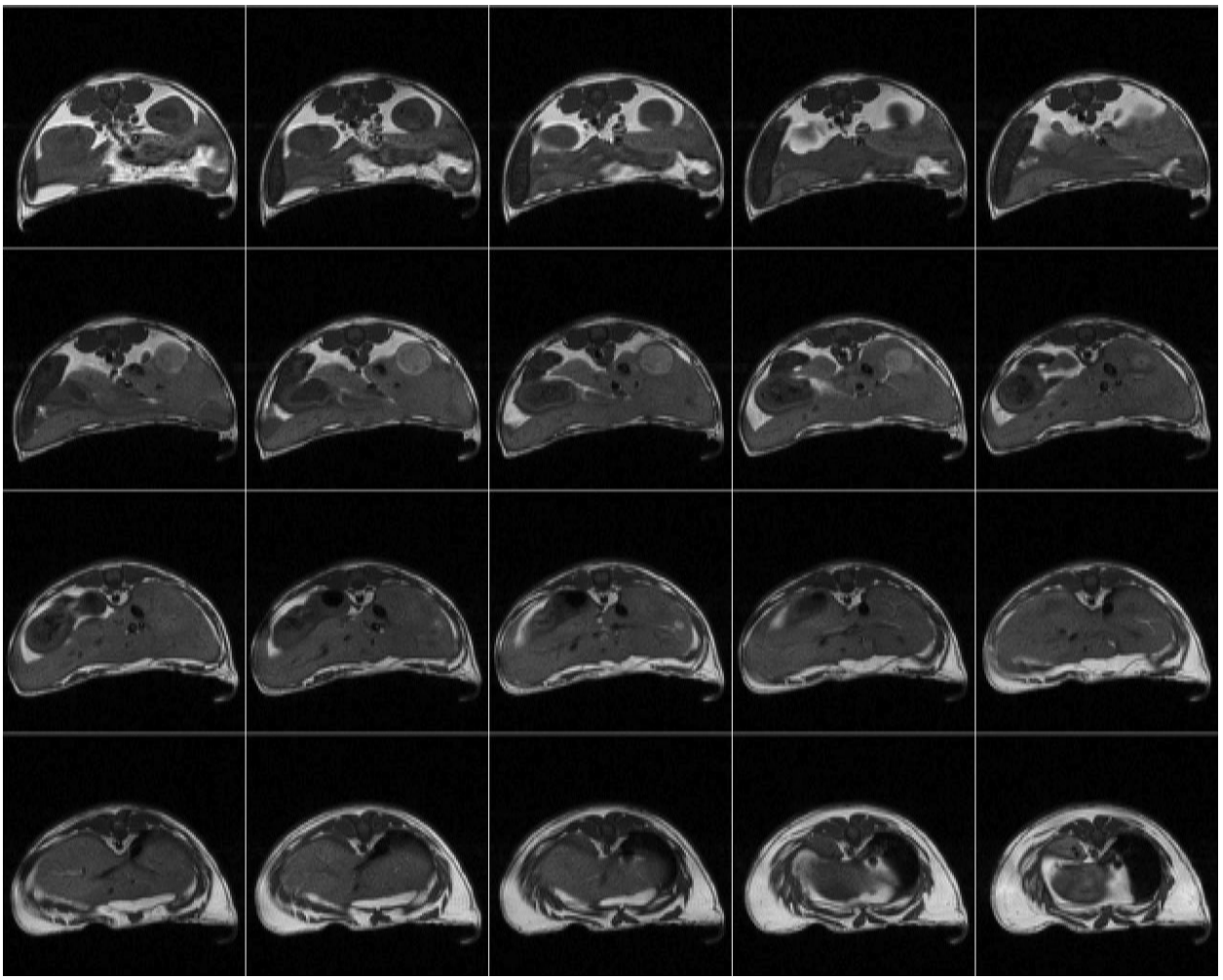

Figure 5.2.1.2. *MRI of a wt mouse*

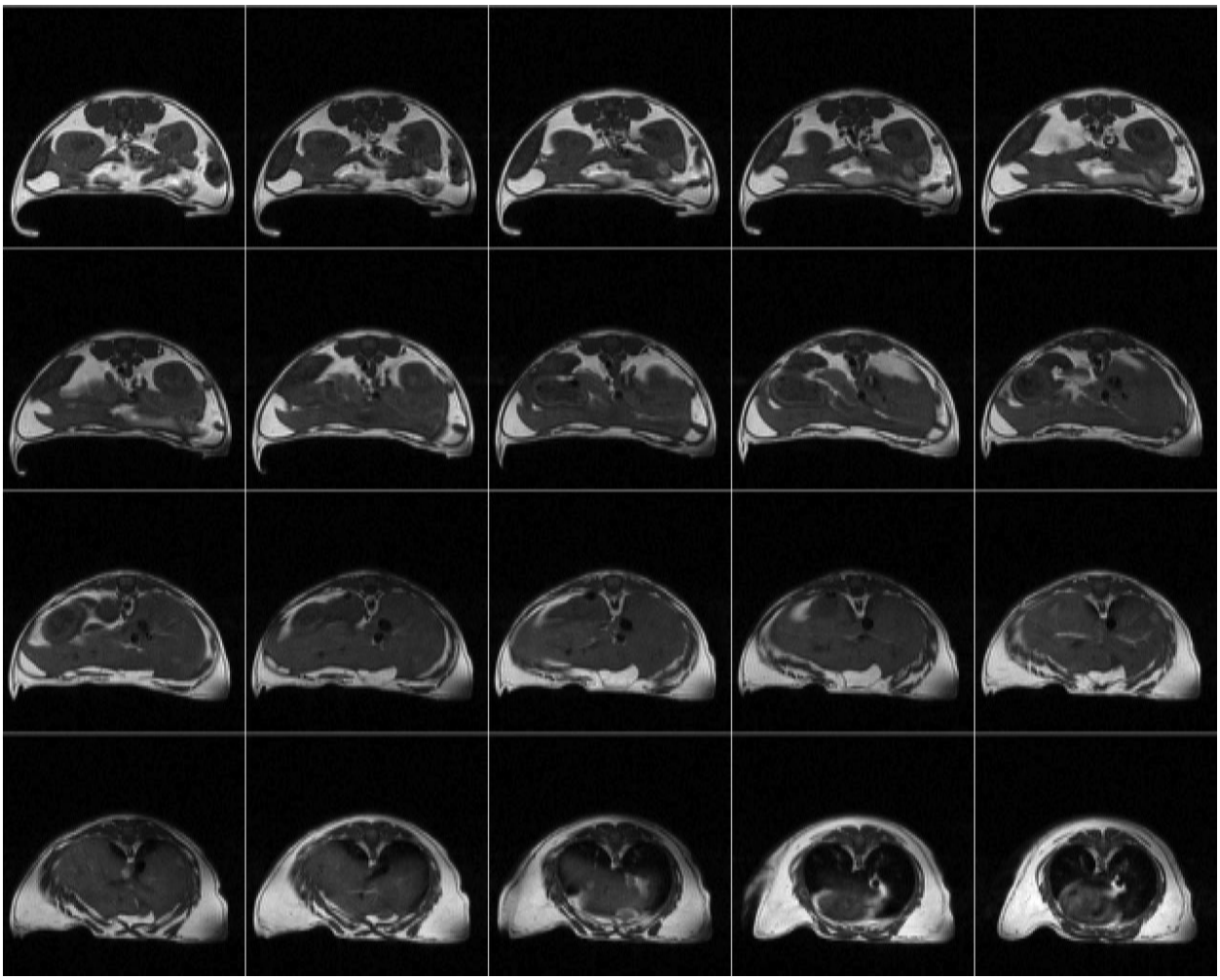

Figure 5.2.1.3. *MRI of a fat-1 mouse*

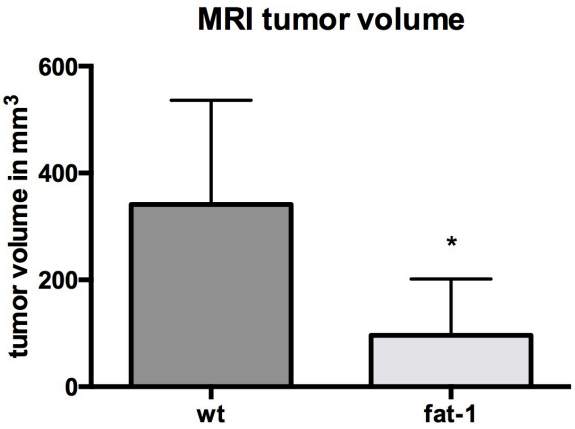

Figure 5.2.1.4. *Significantly reduced mean tumor volume in transgenic fat-1 mice in mm^3 as measured by magnetic resonance imaging. (* $p < 0.05$).*

5.2.2 Macroscopic evaluation of livers

There was no difference in body weight at the time of sacrifice, although the slightly lower body weight in wt mice could be accounted for by a larger tumor burden (Fig. 5.2.2.1). After post mortem removal of the livers, the tumors visible on the organ surface were counted and measured stereomicroscopically. There were significant macroscopically visible differences in the surface tumor load between the two groups of mice: the total number of tumors bigger than 3 mm was significantly lower in the fat-1 mice than in their wt littermates (Fig. 5.2.2.2). There was also a highly significant difference in the largest tumor diameters discernible on the organ surface of each animal, with an average largest diameter of 9.5 mm in wt mice versus only 4.2 mm in fat-1 mice (Fig. 5.2.2.3). Also, we investigated the lungs as the most common site of metastases of HCC and performed structural analysis as well. There were no macroscopically visible metastases in the lungs of either fat-1 or wt mice. Also, microscopically there were no tumor lesions visible in representative H&E stained sections of the lungs.

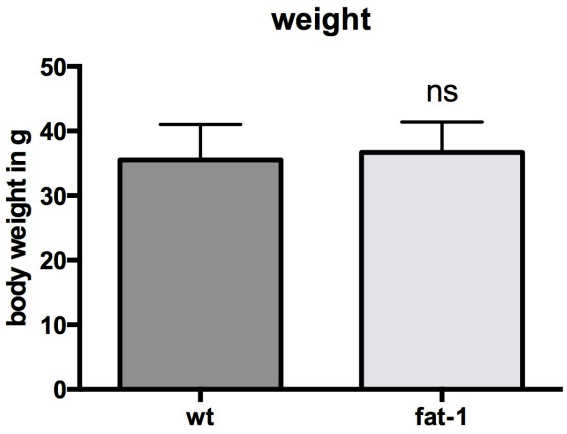

Figure 5.2.2.1. *No difference in body weight between wt and fat-1. (ns = not significant).*

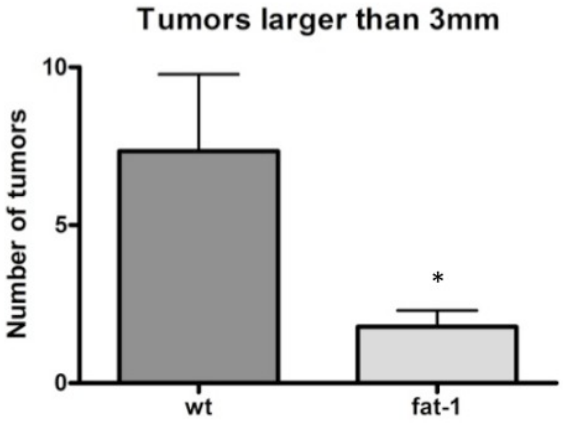

Figure 5.2.2.2. *Tumor count of tumors larger than 3 mm is significantly lower in fat-1 mice. (* p < 0.05).*

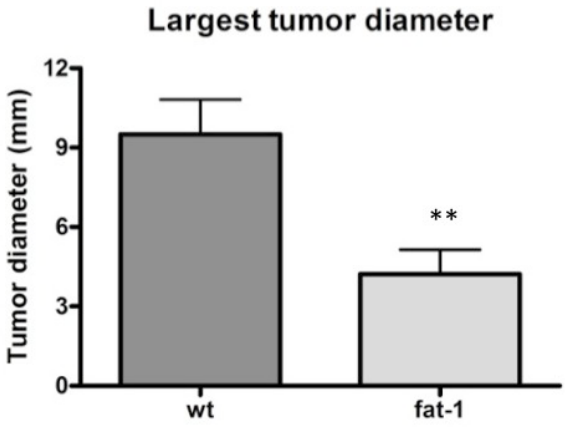

Figure 5.2.2.3. *The diameter of the largest tumor that was superficially visible was significantly smaller in fat-1 mice. (** p = 0.01).*

5.3 Histological evaluation of livers and lungs

The pathological evaluation of hematoxylin and eosin, reticulin- and trichrome-stained slides (Fig. 5.3.1) from the median liver lobe showed a lower number of neoplastic foci in the DEN-treated fat-1 mice compared with the wt mice, although that difference failed to reach statistical significance (Fig. 5.3.2). The microscopically evaluated tumors in the wt group were of grade 2 (moderately differentiated) in three wt mice, with one wt mouse showing grade 3 (poorly differentiated) and only two wt mice were showing grade 1 (well differentiated) tumors. In contrast, there were no neoplastic lesions in the evaluated slides

from two fat-1 mice and only one fat-1 mouse showed a grade 2 (moderately differentiated) lesion, whereas the remaining six fat-1 mice only had grade 1 (well differentiated) lesions. There was no lymphovascular invasion in either group of samples.

Scoring of inflammatory changes indicated more inflammatory changes in the DEN-treated wt animals, as evaluated by necrosis (0 to 4 – absent to confluent necrosis), fibrosis (0 to 4 – absent to cirrhosis), and steatosis (0 to 3 – absent to over 66 % of tissue area). In the wt group, the average score for necrosis was 1 versus 0.33 in the fat-1 group. The fibrosis score was averaged at 0.5 in wt mice and 0.22 in fat-1. Scores for steatosis were 1.5 and 1.22 for wt and fat-1 animals, respectively. However, these differences were not statistically significant (Fig. 5.3.3). We also assessed the area stained with blue dye in the trichrome stain, a routine stain for liver biopsies, representing an increase of collagen in fibrotic or cirrhotic tissues (right panel in Fig 5.3.1), which was significantly lower in fat-1 mice as compared to wt mice (Fig. 5.3.4).

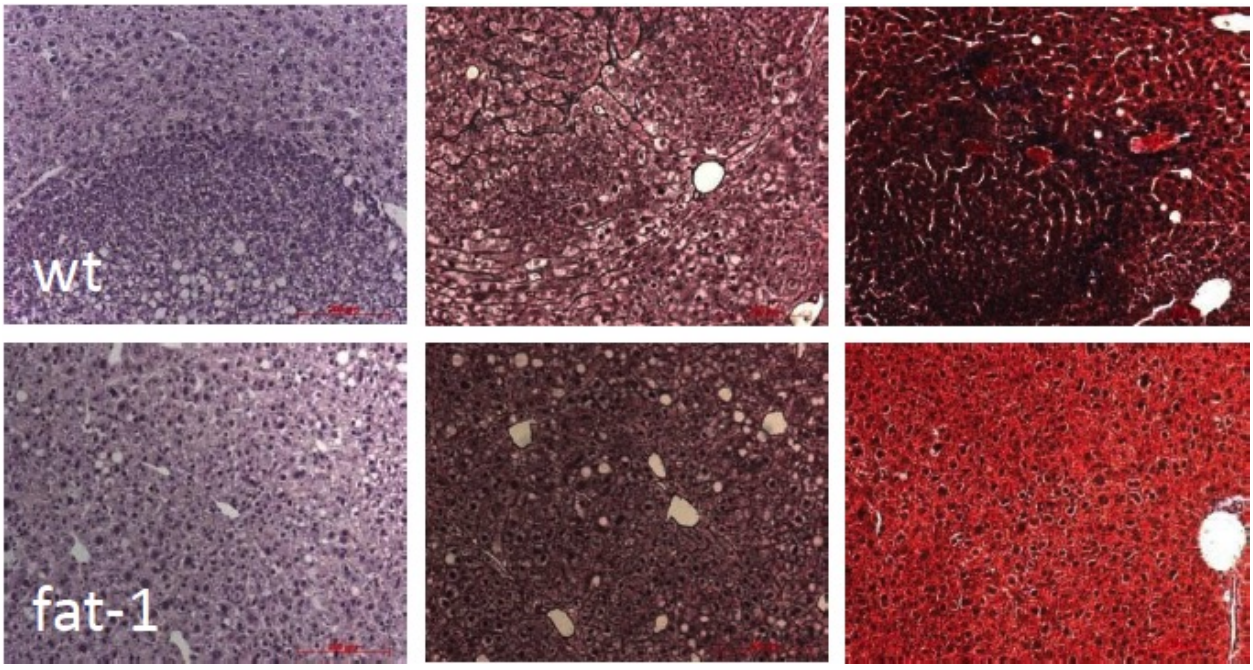

Figure 5.3.1. *Microscopic evaluation of representative hematoxylin and eosin (left) as well as reticulin (middle) and trichrome (right) stains from the median lobe of DEN-treated wt (upper panel) and fat-1 (lower panel) animals. Assessment in trichrome stains confirmed increased connective tissue in livers from wt mice as compared with fat-1 mice.*

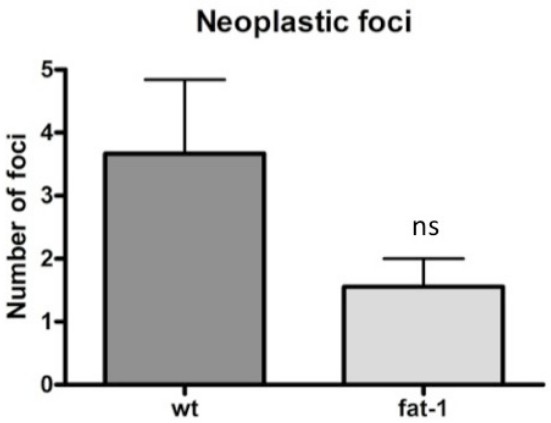

Figure 5.3.2. *There were insignificantly lower numbers of neoplastic foci in fat-1 mice (ns, not significant).*

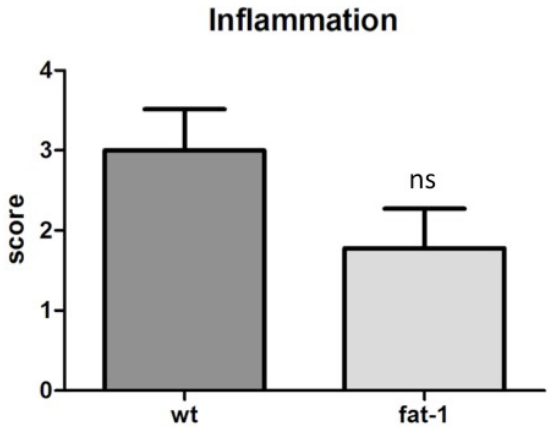

Figure 5.3.3. *Scoring of inflammatory changes indicated more inflammatory changes in the DEN-treated wt animals, however, this difference did not reach statistical significance (ns, not significant).*

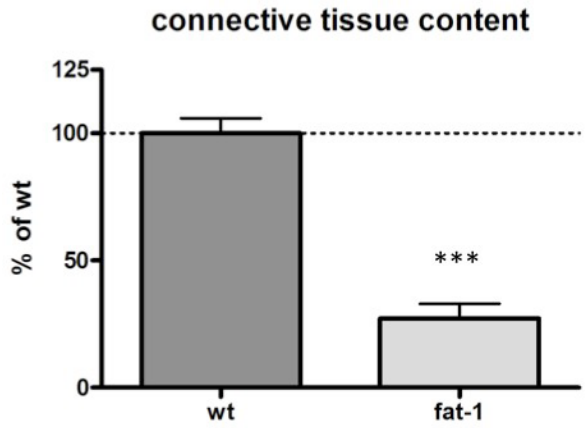

Figure 5.3.4. *The quantity of connective tissue content in comparison of blue connective tissue in trichrome stains was significantly lower in fat-1 vs. wt mice. (*** p = < 0.001).*

5.4 Markers of inflammation in serum, and evaluation of immunohistochemistry

To study the molecular basis for the observed anticancer effect in the fat-1 mice, we measured the levels of TNF-α and COX-2, which are known to play important roles in liver tumorigenesis. We also performed a stain for macrophages, myofibroblasts and endothelial cells in the liver tissue, and measured the levels of ALT and AST in the serum of the DEN-treated animals.

5.4.1 TNF-α

The plasma levels of TNF-α in the fat-1 mice with DEN-induced liver tumors were significantly lower than those in the wt mice (Fig. 5.4.1.1). DEN-treated fat-1 mice had lower levels of plasma transaminases than wt animals with DEN-induced tumors, indicating less severe liver cell damage in the fat-1 mice (Fig. 5.4.1.2).

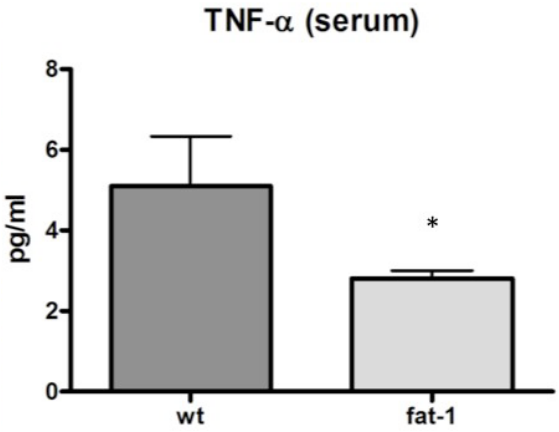

Figure 5.4.1.1. *Assessment of plasma TNF-α shows decreased levels in DEN-treated fat-1 mice as compared to wt animals (* p < 0.05).*

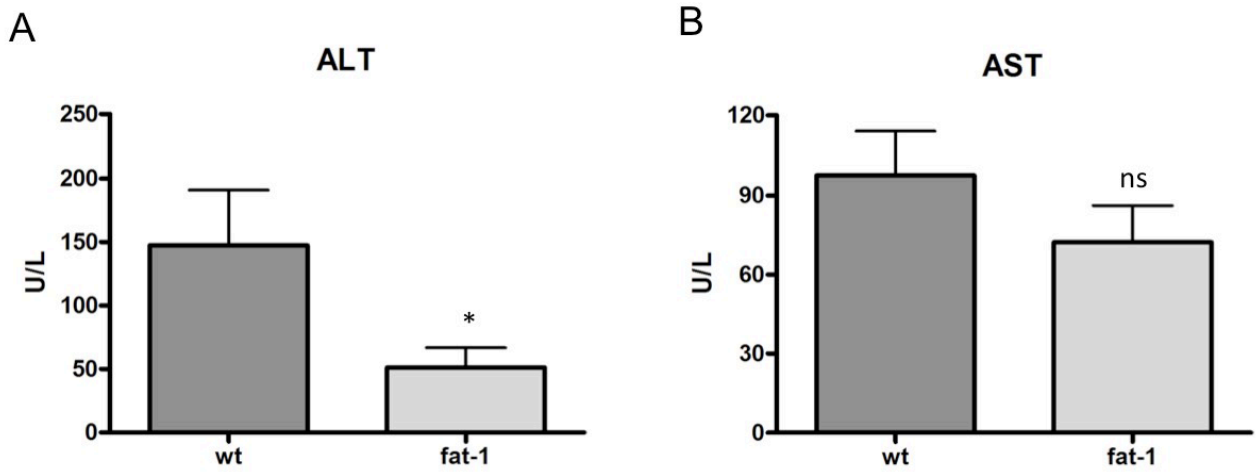

Figure 5.4.1.2. *Assessment of liver damage. Hepatic cell damage as measured by ALT and AST levels in serum was lower in the fat-1 mice as compared to wt mice, graphs are shown for alanine transaminase (**A**) and aspartate transaminase (**B**) (ns = not significant, * p < 0.05).*

5.4.2 COX-2 stain

Immunohistochemical analysis of liver tissue demonstrated higher COX-2 expression in the livers of DEN-treated wt mice compared with fat-1 mice treated with DEN (Fig. 5.4.2.1 and 5.4.2.2), supporting the inflammation dampening effect observed in fat-1 mice.

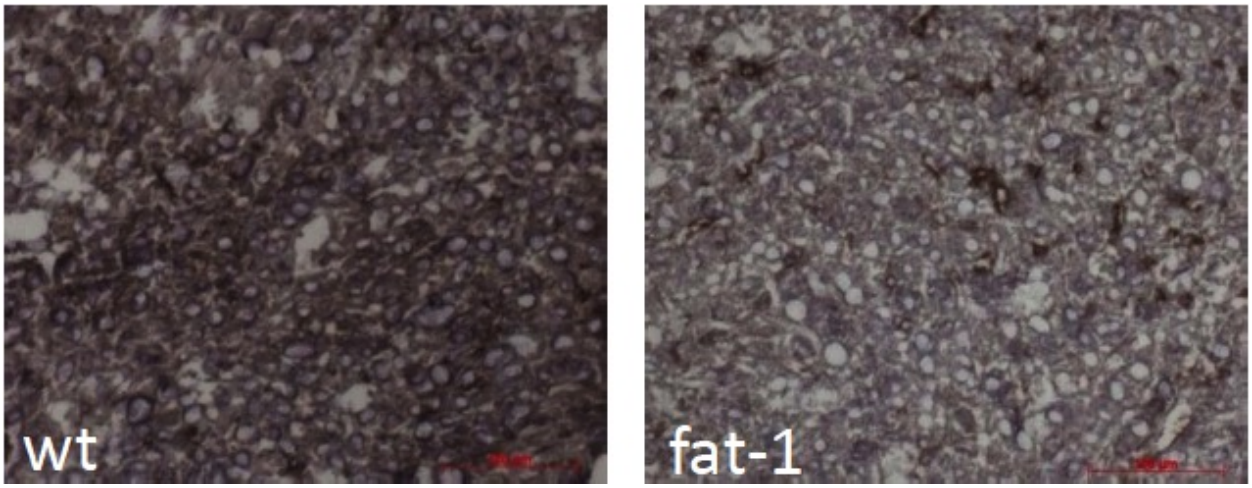

Figure 5.4.2.1. *Hepatic COX-2 expression in wt (left) and fat-1 (right) mice with DEN-induced liver tumors.*

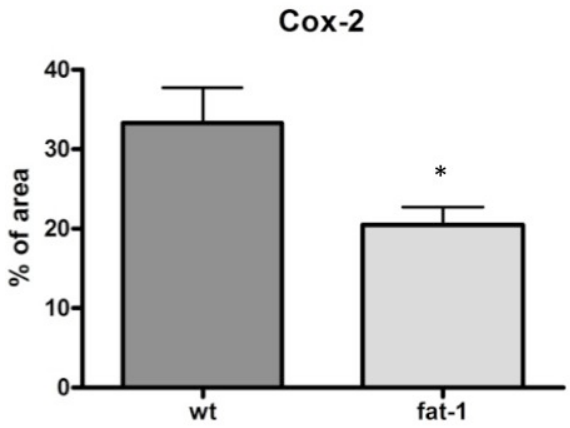

Figure 5.4.2.2. *The protein expression of COX-2 in the livers of DEN-treated mice was significantly lower in fat-1 compared to wt mice (* $p < 0.05$).*

5.4.3 Staining of macrophages (F4/80 positive)

While there were macrophages discernible in slides from four of five assayed wt mice (Fig. 5.4.3 A), no macrophages were detectable in the slides from the seven assayed fat-1 mice (Fig. 5.4.3 B).

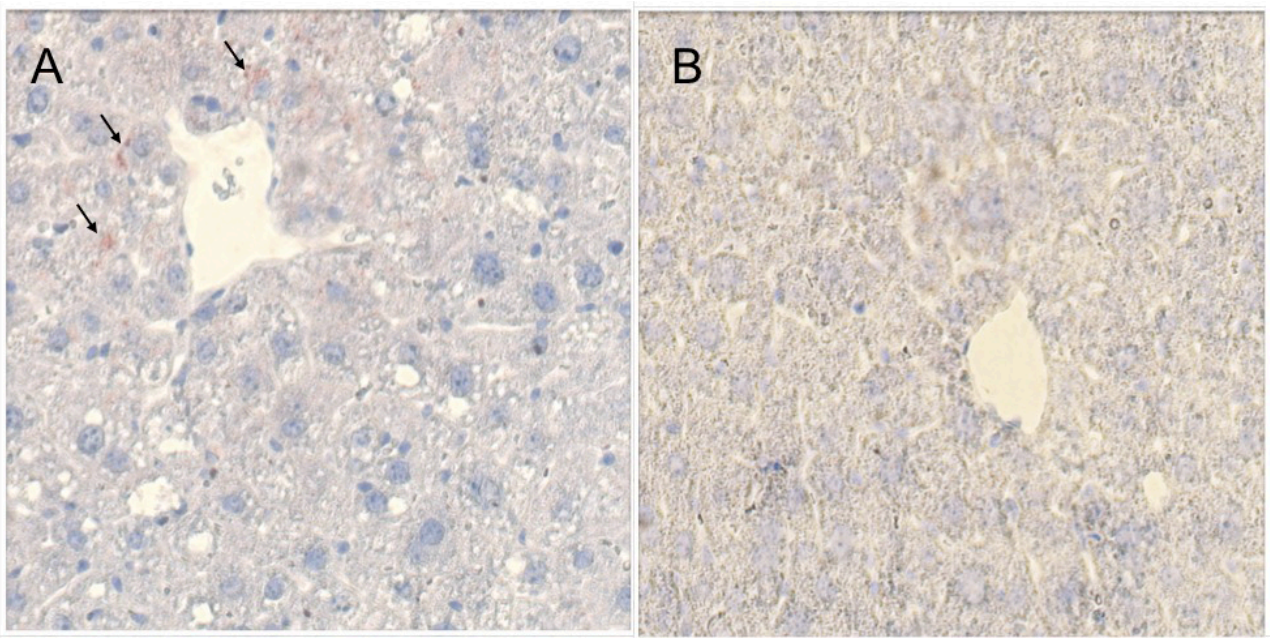

Figure 5.4.3. *Analysis of F4/80-expression in DEN-treated animals demonstrated intraparenchymal macrophages (several are indicated by arrows) in most wt mice (**A**), while there were no F4/80-positive cells discernible in the fat-1 mouse samples assayed (**B**).*

5.4.4 Evaluation of fibrosis

In order to further examine the effect of the different n-3 PUFA tissue content on liver pathology, staining for α-SMA to visualize myofibroblasts and activated hepatic stellate cells (reflecting fibrogenic activity) in the livers of DEN-treated animals was performed and showed a significantly lower number of these cells in liver tissue from fat-1 mice (Fig. 5.4.4). In line with this finding, a significantly decreased connective tissue content in the fat-1 livers was documented in the trichrome stains as described above (Fig. 5.3.1).

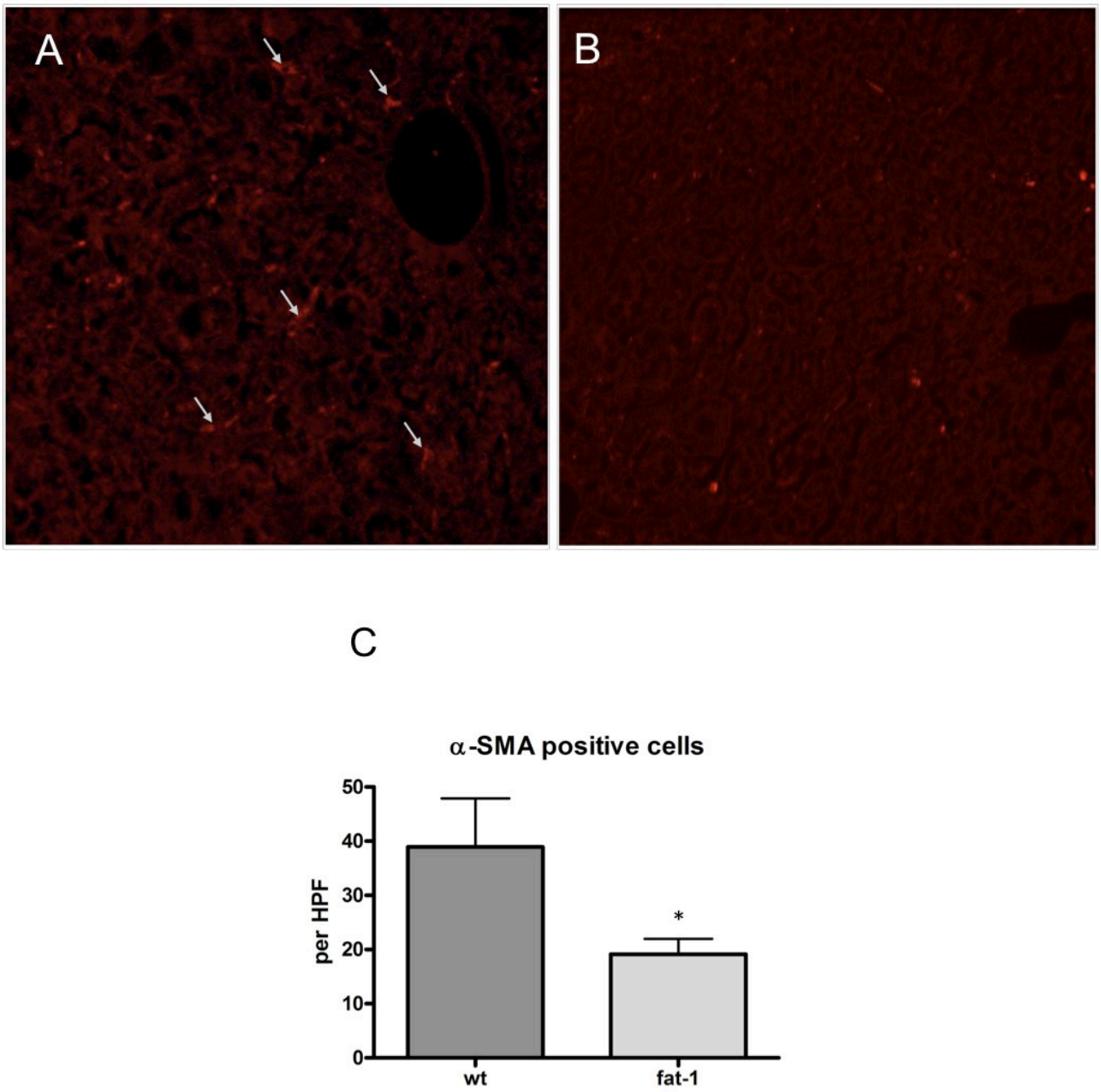

Figure 5.4.4. *Indications of decreased hepatic fibrogenesis in fat-1 mice. Wt mice **(A)** showed significantly more α-SMA-positive activated hepatic stellate cells and myofibroblasts (some indicated by arrows) than fat-1 mice **(B)** as quantified in the slides (**C**) (* $p < 0.05$).*

5.4.5 Neovascularization

Staining of CD31 positive endothelial cells in liver tumors of wt and fat-1 mice was performed to determine intratumoral microvascular density. Although there was more angiogenesis noted in wt liver tumors, this difference did not reach statistical significance (Fig. 5.4.5).

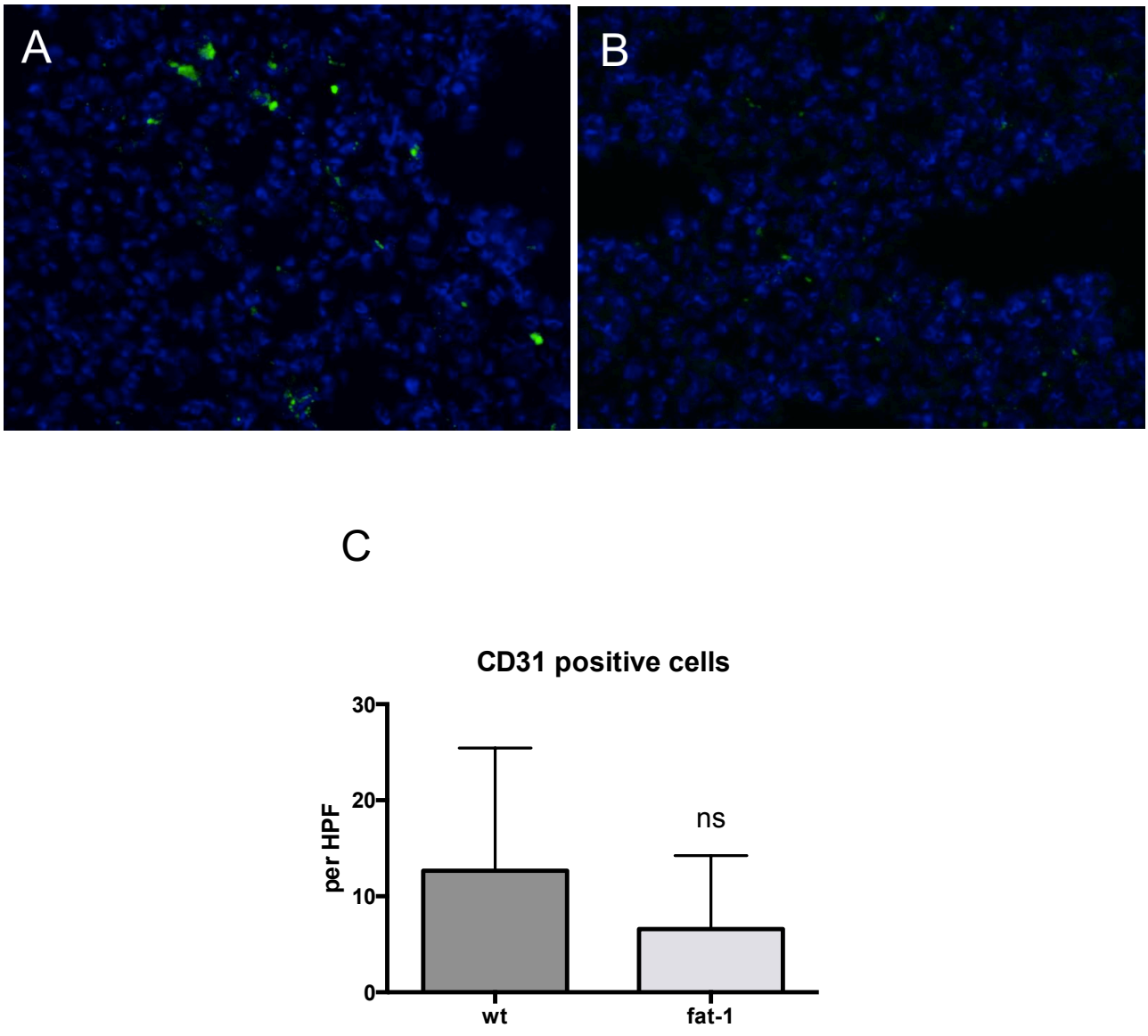

Figure 5.4.5. *Angiogenesis measured by CD31: There was no difference in the level of angiogenesis in the livers of DEN-treated mice (**A**) wild type, (**B**) fat-1, as measured by CD31-positive cells (**C**) (ns = not significant).*

5.5 Expression of NFκB

The levels of the pro-inflammatory transcription factor NFκB were measured in the livers of DEN-treated fat-1 and wt mice to interpret their role in cancer development. However, the difference was not significant (Fig. 5.5.1).

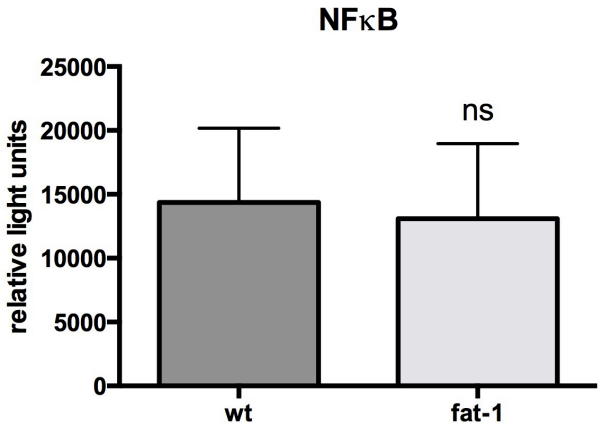

Figure 5.5.1. *Hepatic NFκB content: There was no significant difference detectable in the level of NFκB in the livers of DEN-treated fat-1 mice as compared to wt animals (ns = not significant).*

5.6 Formation of n-3 derived anti-inflammatory mediators

The profile of lipid mediators formed from PUFA was determined by Dr. rer. medic. Beate Gomolka and Dr. rer. nat. Michael Rothe in samples supplied by me. To assess the concentrations of lipid mediators, we used liquid chromatography-coupled tandem mass spectrometry. Analysis focused on the n-3 PUFA-derived mono-hydroxylated compounds 18-HEPE (derived from EPA) and 17-HDHA (derived from DHA) as well as the n-6 PUFA-derived 15-HETE (from AA). There was a highly significant difference in the liver tissue concentrations of 18-HEPE and 17-HDHA between fat-1 and wt mice. For 18-HEPE, tissue levels were 18.5 + 3.1 ng/g in fat-1 mice vs. non-detectable levels in wt mice (Fig. 5.6 A and C), for 17-HDHA, tissue levels in fat-1 mice reached 326.9 + 38.3 ng/g vs. 72.6 + 23.9 ng/g in wt mice Fig. 5.6 B and D). Compared to the baseline DHA levels in livers of fat-1 and wt animals, the 4.5-fold increase in 17-HDHA in fat-1 mice over wt mice compares with

4.2-fold higher tissue levels of DHA in fat-1 over wt mice. There were no significant differences in the 15-HETE levels between the two groups of mice.

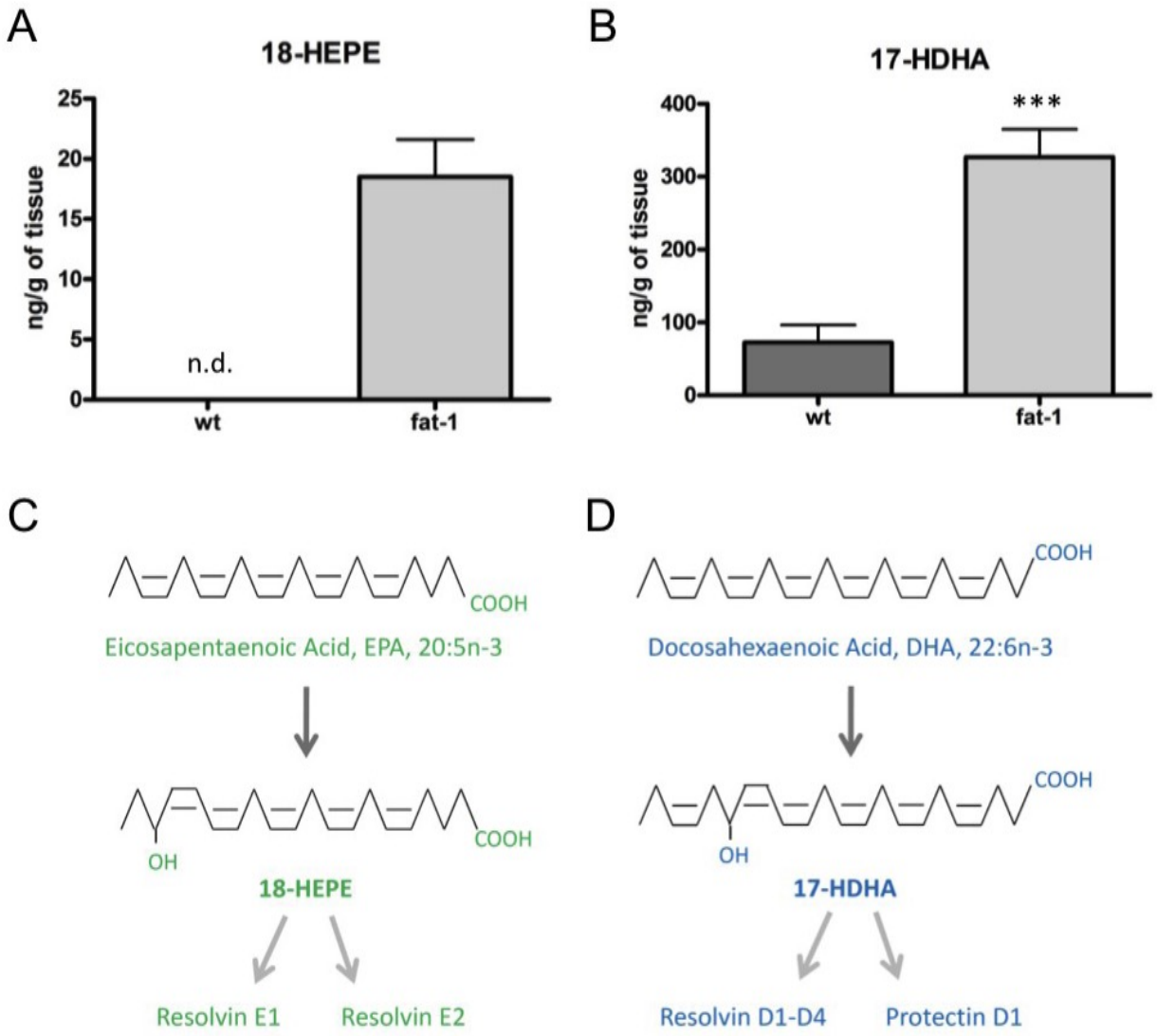

Figure 5.6. *Formation of 18-HEPE from EPA (**A** and **C**) and of 17-HDHA from DHA (**B** and **D**) is increased in liver tissue from fat-1 mice with DEN-induced tumors as compared to DEN-treated wt animals. 18-HEPE and 17-HDHA could contribute to an anti-inflammatory effect themselves and also be further metabolized to anti-inflammatory resolvins and protectins as shown in (**C**) and (**D**) (*** $p < 0.001$).*

6 Discussion

Hepatocellular carcinoma (HCC) is a major cause of morbidity and mortality worldwide. The development of HCC is mostly associated with chronic inflammatory liver disease of various etiologies. Previous studies have shown that omega-3 (n-3) polyunsaturated fatty acids (PUFA) dampen inflammation in the liver and decrease formation of tumor necrosis factor (TNF)-α.

In this study, we used the fat-1 transgenic mouse model, which endogenously forms n-3 PUFA from n-6 PUFA to determine the effect of an increased n-3 PUFA tissue status on tumor formation in the diethylnitrosamine (DEN)-induced liver tumor model.

Our results showed a decrease in tumor formation, in terms of size and number, in fat-1 mice compared with wild-type littermates. Plasma TNF-α levels and cyclooxygenase-2 expression were markedly lower in fat-1 mice. However, there was no difference in NFκB activity in the liver tissue of fat-1 versus wt animals. A parameter for the degree of liver cell damage, blood ALT was higher in the wt mice as compared to their fat-1 littermates. COX-2 expression was higher in wt mice as compared to fat-1 mice. We also performed staining for α-SMA in order to visualize activated hepatic stellate cells and thus fibrogenic activity in the livers of the examined animals. There was a significantly lower number of positive cells in liver tissue from fat-1 mice.

Lipidomics analysis of lipid mediators revealed significantly increased levels of the n-3 PUFA-derived 18-hydroxyeicosapentaenoic acid (18-HEPE) and 17-hydroxydocosahexaenoic acid (17-HDHA) in the livers of fat-1 animals treated with DEN.

The results of this study provide evidence that an increased tissue status of n-3 PUFA suppress liver tumorigenesis, probably through inhibiting liver inflammation. The findings also point to a potential anticancer role for the n-3 PUFA-derived lipid mediators 18-HEPE and 17-HDHA, which can down-regulate the important pro-inflammatory and proliferative factor TNF-α.

In other disease models, e.g. dextran sodium sulfate (DSS)-induced colitis, protection from colitis in fat-1 mice also involved decreased NFκB activity and decreased expression of TNF-α, and decreased PGE_2 levels (62, 83).

6.1 Animals (fat-1 model and fatty acid profiles of liver tissue)

A vast amount of studies have shown evidence that the n-3 PUFAs rich in fish oil, such as DHA and EPA, prevent carcinogenesis (84, 85). Several studies have examined the role of fish oil fatty acids in cell cultures, rat models of hepatic carcinogenesis as well as in the fat-1 mouse model. In vitro experiments showed that DHA and EPA were able to inhibit the growth of three human HCC cells (Hep3B, Huh-7, HepG2) (75). A study with 7,12-dimethylbenzanthracene-induced liver tumors in rats showed that a diet rich in fish oil leads to a decrease of PGE_2 concentrations in livers and liver tumors. However, there was no decreased tumor incidence as compared with an evening primrose oil-treated group (86). Other studies found decreased formation of hepatic neoplastic foci in fish oil-treated rats with DEN-induced hepatocarcinogenesis (87, 88). Fat-1 mice were recently used in a genetic hepatoma model in mice containing mutations in c-myc and TGF-α (transforming growth factor alpha) (74), as well as in an inoculation liver tumor model (75). Both models demonstrated significant anti-tumor activity in the fat-1 mice. However, both studies focused primarily on protein analysis, notably demonstrating lower NFκB and COX-2 expression in the fat-1 livers, respectively. Analysis of n-3 PUFA lipid mediators was not performed so far.

Overall, use of the fat-1 model is a better means of comparing omega-3 influence on pathogenesis than feeding omega-3 because one can rule out the confounding factor of diverging diets with differing ingredients.

Inducing inflammation and HCC in mice by DEN injection is a more realistic model in the translation to human disease pattern than triple mutant mice or inoculation models. Multiple studies comparing mouse models of liver cancer discussed that comparative functional genomics showed that the gene expression patterns in HCCs in DEN induced mouse liver cancers were most similar to those of human HCCs (39, 89).

Anthropological and epidemiological research and studies at the molecular level showed that human beings evolved on a diet with omega-3 to omega-6 ratios of approximately 1:1 whereas the modern Western diet represents more a ratio of 1:10-1:25. This ratio is thought to be part of the pathogenesis of multiple inflammatory and neoplastic diseases (90). The fatty acid profiles of liver tissue of fat-1 mice demonstrate PUFA ratios similar to those of our human ancestors, the PUFA content of livers of wt mice is representative of a typical contemporary Western diet.

6.2 Assessment of tumor incidence and tumor load

The results of this study demonstrate a significantly decreased hepatic tumorigenesis in fat-1 mice with endogenously increased tissue n-3 PUFA levels. This is in congruence with a study performed by Lim et al. in 2009, showing markedly smaller tumors in fat-1 mice compared to wt mice in a murine HCC inoculation model with Hepa1-6 cells (75).
This study has some limitations, however, due to the focus on the biochemical analysis of liver tissue, systematic histological workups of whole mouse livers to differentiate between malignant and benign tumors were not done. To evaluate the exact extent of tumor formation, it would be ideal to perform MRI, and compare it to post-mortem macroscopic and microscopic analysis of whole mouse livers, but a direct histological assessment of size and number of lesions in serial sections was not performed, because our other experiments required different processing of the tissue. Furthermore, due to the low tumor load in DEN-treated fat-1 animals, comparative measurements from isolated tumor tissue were not performed.

6.2.1 MRI

The use of MRI to assess each mouse's tumor burden was a useful in vivo tool. The resolution of our 4.7 T small animal MRI was possibly not high enough to catch small tumors. In future studies, one could also include the scanning of the lungs to evaluate for possible metastases. Moreover, we found in our MRI experiments that the fat content is not the same in each detected tumor and might represent different tumor subtypes or entities, which might be better evaluated by also performing MR spectroscopy. The observed different tumor densities could also represent regenerative nodules (benign tumors).

6.2.2 Macroscopic evaluation of livers

Counting and measuring the surface tumors under stereomicroscopy yields a comparison that is thought to be indicative of the overall tumor burden. It is difficult to take all minute little tumors into account and our cut-off size was 0.5 mm.
The weak point of the macroscopic evaluation of the livers is that only surface tumors can be counted and measured but they might not be representative of the total tumor

burden. It is thus advisable to combine the 3 modalities of MRI, macroscopic and microscopic evaluations.

We found in our study, that the diameters of tumors of wt mice were larger than the tumors of fat-1 mice. Interestingly, a multi-centered cohort study examining the diameter of largest tumor, number of nodules and vascular invasion on post explant livers and correlating this to post transplant survival and recurrence found also that the diameter of the largest tumor was a more important predictor of survival and recurrence than the number of nodules (91).

6.3 Microscopic evaluation of livers and lungs (H&E, reticulin, trichrome; scoring)

The decreased hepatic tumorigenesis in fat-1 mice was associated with decreased inflammation/regeneration and fibrosis as observed by a blinded pathologist. Reticulin and trichrome stains were performed to better evaluate the development of fibrosis, which is a crucial factor in HCC development in humans. A recent study performed by Bogaerts et al. in 2015 also used the reticulin stain to assess liver fibrosis and cirrhosis to evaluate the influence of hypoxia on HCC tumor progression (92). Another group also used a trichrome stain to assess fibrosis in a knockout mouse model studying hepatocarcinogenesis (93). To our knowledge, no research has been published yet using all three staining methods to compare fibrosis, cirrhosis and hepatocarcinogenesis in a DEN induced HCC mouse model.

The microscopic evaluation would ideally be done of the entire liver to be able to compare tumor burden detected histologically with externally visible tumors and calculated MRI tumor volumes, but it would then not leave tissue for processing for other biochemical examinations.

6.4 Markers of inflammation in serum and evaluation of immunohistochemistry

In fat-1 mice, inflammation markers such as TNF-α and COX-2 were decreased as compared to wt littermates and intrahepatic macrophages as well as decreased activated hepatic stellate cells and myofibroblasts were found. These data confirm

previous observations in the D-GalN/LPS model of acute hepatitis (61) and are consistent with other findings showing that mice fed with DHA-enriched diets in a CCl_4-induced hepatitis model had a significant decrease in COX-2 mRNA expression and inflammatory response (59). A recent study showed that n-3 PUFA inhibited HCC cell growth through blocking β-catenin and COX-2 and reduced tumor formation of inoculated hepatoma cells in fat-1 mice (75). Studies by Gonzalez-Periz et al. and in our laboratory using murine macrophage cell lines showed suppression of LPS-triggered TNF-α secretion by 17-HDHA and 18-HEPE (59).

6.4.1 TNF-α levels in serum

In a D-GalN/LPS model of an acute hepatitis, less severe inflammatory liver injury in fat-1 mice with a balanced n-6/n-3 PUFA ratio was demonstrated. This decreased inflammatory response was associated with decreased plasma TNF-α levels in fat-1 mice (94). Gonzalez-Periz et al. also demonstrated a direct anti-inflammatory effect of 17-HDHA by inhibition of TNF-α secretion from macrophages in vitro, arguing towards a critical role for n-3 PUFA-derived lipid mediators in the dampening of inflammation in the liver (59). In the context of tumorigenesis there is also an important role for TNF-α in the liver. A recent study showed that increased DEN-induced carcinogenesis is probably due to sustained c-Jun N-terminal kinase (JNK) activation in cells exposed to TNF-α, leading to increased compensatory proliferation of surviving hepatocytes (15). In the data presented here, we found decreased TNF-α activity in the fat-1 mice arguing for a less pronounced pro-proliferative signaling in the livers of treated animals in this study and thereby preventing the hyperproliferation associated with DEN treatment in wt mice. This was associated with a highly significant increase in 17-HDHA formation in liver tissue from fat-1 animals, which could be an important factor suppressing TNF-α formation from macrophages. While 17-HDHA and other omega-3 derived lipid mediators were shown to be important anti-inflammatory and pro-resolution factors, our data indicate that they can also suppress tumorigenesis via suppression of TNF-α formation, underscoring the potential importance of omega-3 fatty acids in the suppression of tumorigenesis.

6.4.2 ALT and AST levels in serum

ALT and AST are non-specific markers of hepatic injury. They were elevated in both study groups, representing general damage to the DEN-treated livers, and were less elevated in fat-1 mice, pointing towards a protective effect, although the differences for AST were not significant. This is in line with findings in a D-GalN/LPS induced hepatitis model, where ALT levels in the serum of fat-1 mice were significantly lower than in wt mice (61).

6.4.3 Immunohistochemistry (COX-2, F4/80, α-SMA, CD31)

Hepatic inflammation and neoplasia are in part promoted by COX-2 activation and production of PGs from AA (95). Treatment with aspirin and other NSAIDs decreased the incidence of esophageal, colorectal, bladder, lung, and gastric cancers, indicating the significance of COX-2 in many malignancies (96). PGE_2 has been shown to be associated in multiple stages of tumorigenesis like modulation of inflammation, cancer cell proliferation, differentiation, apoptosis, angiogenesis, metastasis, and host immune response to cancer cells (95). Gonzalez-Periz et al. demonstrated that mice that were fed DHA-enriched diets had a significant decrease in hepatic COX-2 mRNA expression and decreased inflammatory changes (59). Recent findings suggested that DHA inhibits the expression of COX-2 through suppression of gene transcription, and COX-2 was linked to inhibiting HCC growth by blocking COX-2 signaling pathways, especially COX-2-derived PGE_2 (75). DHA and EPA treatment of Hep3B cells induced a reduction of cell viability, whereas DHA and EPA had no cytotoxic effect in primary cultures of liver parenchymal cells (75). These findings are in concurrence with our results, a decrease in COX-2 expression in fat-1 mice was associated with a decreased tumor burden. One limitation of our study was that we were not able to accurately perform a Western blot of COX-2, but only did immunohistochemistry. In future studies, this technique should also be used to yield more accurate results.

We also performed an F4/80 stain as a marker of macrophage invasion, which showed intraparenchymal macrophages in most wt mice, but none discernible in the examined fat-1 mouse samples. This finding is in agreement with multiple other studies that identified an inflammation dampening effect of n-3 PUFA on macrophages (97, 98). Fibrogenesis was reduced in DEN-treated fat-1 mice as compared to wt mice, as detected by significantly less α-SMA-positive hepatic stellate cells and myofibroblasts in

fat-1 mice. A recent study by Weylandt et al. also found a decreased amount of activated pancreatic stellate cells in a cerulein induced chronic pancreatitis model in the fat-1 mouse, arguing for a genuine inhibition of fibrosis in chronic inflammation (99).
HCC is a highly vascular tumor with high levels of VEGF, which have recently been the target of treatment with Sorafenib. Consequently, higher levels of VEGF or CD31 as a marker of endothelial cells and thus of neovascularization would be an indicator of higher tumor burden. Our study failed to show a difference in the amounts of CD31-positive cells. In future experiments, one should measure VEGF by Western blot.

6.5 NFκB-ELISA of liver tissue

NFκB regulates the transcription of a myriad of genes involved in immune response, cell adhesion, differentiation, proliferation, angiogenesis and apoptosis. However, variants in the genes coding for NFκB and IκB proteins were not associated with HCC development in patients with chronic hepatitis B (100). A study with a transgenic liver tumorigenesis approach demonstrated a lower tumor incidence in triple-mutant c-myc/transforming growth factor-alpha/fat-1 mice with a significant decrease in NFκB protein levels in the fat-1 group and alterations in gene expression patterns (74). In some studies, NFκB inhibition promotes carcinogenesis, but in others, NFκB suppressed cancer promotion and development (69). These opposing results might be explained by a study by Maeda et al. who demonstrated that NFκB activity in Kupffer cells contributes to hepatocarcinogenesis and that NFκB activity in hepatocytes acts as a cancer suppressor (16). We did not find a difference in NFκB activity between DEN-treated liver tissues from fat-1 or wt animals.

6.6 Analysis of PUFA and lipid mediators

In this study, we show that an increased tissue content of omega-3 fatty acids in the liver can suppress chemically induced hepatocellular tumorigenesis. Omega-3 fatty acids have been implicated in the context of inflammation dampening, and multiple previous studies with fat-1 mice demonstrated decreased inflammation-associated colon carcinogenesis (101), protection from colitis (62), acute hepatitis (61), diet-

induced non-alcoholic fatty liver disease (102), pancreatitis (99) and allergic airway responses (103) due to the increased n-3 PUFA content in these mice.

Many studies have also described a role for omega-3 fatty acids in the (competitive) inhibition of the formation of AA-derived lipid mediators. In the context of tumor cell growth, recent studies have identified AA-derived cytochrome P450 metabolites, the epoxyeicosatrienoic acids (EET), as pro-proliferative factors in tumor cells leading to activation of MAP kinases and the PI3 kinase-AKT system (104). EET treatment was able to promote tumor metastasis, and cytochrome P450 overexpression enhanced metastatic potential and tumor angiogenesis in another study (105). EETs were shown to participate as second messengers in the angiogenic response initiated by VEGF (106). In the data presented here, we show that endogenously increased omega-3 fatty acids in the fat-1 mouse lead to the formation of fewer as well as smaller liver tumors. This could be an effect of the decreased formation of EETs in these mice.

The n-3 PUFAs EPA and DHA were significantly higher in fat-1 mice, where the levels of the n-6 PUFA AA in liver tissue did not reach statistical significance. To further evaluate the lipid mediators derived from n-3 and n-6 PUFAs, liquid chromatography tandem mass spectrometry analysis (LC-MS/MS) was performed. As mentioned above, I only supplied the samples, but did not perform LC-MS/MS myself.

The results presented here demonstrate significantly higher levels of the EPA metabolite 18-HEPE and the DHA metabolite 17-HDHA in the livers of fat-1 mice with DEN-induced tumors. While the possibility of auto-oxidation processes leading to the increased 18-HEPE and 17-HDHA levels cannot be excluded, it is regardless of the metabolic pathway leading to their formation that these compounds might contribute a significant biological effect by decreasing TNF-α secretion from macrophages as shown by an in vitro model of other members of our research group (107). To understand the physiological effects of the lipid metabolites 18-HEPE and 17-HDHA, they tested their ability to decrease TNF-α secretion from immune cells. 18-HEPE and 17-HDHA significantly decreased LPS-induced TNF-α secretion from RAW 264.7 murine macrophages. 18-HEPE and 17-HDHA could thereby dampen the inflammatory and regeneratory stimulus and thus, inflammation triggered tumorigenesis in the livers of fat-1 mice. 17-HDHA has previously been described as an anti-inflammatory compound in the context of experimental liver inflammation (59), was confirmed by this study and this approach was extended to the EPA metabolite 18-HEPE. A study performed in Japan

by J. Endo et al. used the fat-1 mouse model to examine the effect of 18-HEPE on pressure overload-induced maladaptive cardiac remodeling. 18-HEPE was shown to inhibit the macrophage-mediated pro-inflammatory activation of cardiac fibroblasts in culture, and a dose-dependent suppression of IL-6 production from cardiac fibroblasts exposed to 18-HEPE was observed (108).
As 18-HEPE and 17-HDHA are the precursors of protectins and resolvins, which have been reported to be potent anti-inflammatory lipid mediators (109), it is also possible that increased levels of 18-HEPE/17-HDHA contribute to anti-inflammatory effects through their conversion to protectins and resolvins. Another possibility is that the increased levels of 17-HDHA in the livers of DEN-treated fat-1 mice could be an indicator of increased formation of the instable intermediate peroxy-metabolite 17-HpDHA, which was shown to be directly cytotoxic to fast-growing tumor cells (110), an effect that might contribute to an antitumor effect beyond the described mechanism of lowering the TNF-α levels.

In light of the data presented here, further work will now be necessary to delineate changes in lipid mediator formation in the context of liver pathologies in different stages and in the context of dietary differences in the uptake of n-3/n-6 fatty acids.

6.7 Conclusion and impact of the study/clinical relevance

Taken together, our study adds new insight to the protective role of n-3 PUFA in liver disease. n-3 PUFA might function as direct antagonists of AA or as upstream suppressors of COX and LOX enzyme expression (45). The data presented here indicate that n-3 PUFA might suppress liver tumorigenesis due to a significant anti-TNF-α effect that is mediated through their hydroxylated metabolites 18-HEPE and 17-HDHA. This, together with the previous *in vitro* and animal studies, provides a strong rationale for the potential application of n-3 PUFA supplementation in the alleviation of chronic liver inflammation and prevention of inflammation-triggered liver tumorigenesis for patients. A balanced fatty acid status in the human diet or dietary supplementation with n-3 PUFA adds further beneficial effects, such as a cardioprotective effect and decrease in colon carcinogenesis, in addition to its possible prevention of HCC development.
More chemo-preventive trials to elucidate the relationship between the formation of n-3 derived lipid mediators and hepatic carcinogenesis using lipidomics should be

performed. Further research is warranted to assess the n-3/n-6 PUFA status and lipid profiles in patients with chronic hepatitis before and during prophylactic intervention with n-3 PUFA dietary supplementation in regards to development of HCC.

7 References

1. Parkin DM. 2001. Global cancer statistics in the year 2000. Lancet Oncol 2:533-543.
2. El-Serag HB, Rudolph KL. 2007. Hepatocellular carcinoma: epidemiology and molecular carcinogenesis. Gastroenterology 132:2557-2576.
3. Greene ER, Huang S, Serhan CN, Panigrahy D. 2011. Regulation of inflammation in cancer by eicosanoids. Prostaglandins Other Lipid Mediat 96:27-36.
4. Mantovani A. 2005. Cancer: inflammation by remote control. Nature 435:752-753.
5. El-Serag HB. 2004. Hepatocellular carcinoma: recent trends in the United States. Gastroenterology 127:S27-34.
6. Rudolph KL, Chang S, Millard M, Schreiber-Agus N, DePinho RA. 2000. Inhibition of experimental liver cirrhosis in mice by telomerase gene delivery. Science 287:1253-1258.
7. Yu MW, Chen CJ. 1993. Elevated serum testosterone levels and risk of hepatocellular carcinoma. Cancer Res 53:790-794.
8. Yu MW, Yang YC, Yang SY, Cheng SW, Liaw YF, Lin SM, Chen CJ. 2001. Hormonal markers and hepatitis B virus-related hepatocellular carcinoma risk: a nested case-control study among men. J Natl Cancer Inst 93:1644-1651.
9. Hassan MM, Frome A, Patt YZ, El-Serag HB. 2002. Rising prevalence of hepatitis C virus infection among patients recently diagnosed with hepatocellular carcinoma in the United States. J Clin Gastroenterol 35:266-269.
10. Freeman AJ, Dore GJ, Law MG, Thorpe M, Von Overbeck J, Lloyd AR, Marinos G, Kaldor JM. 2001. Estimating progression to cirrhosis in chronic hepatitis C virus infection. Hepatology 34:809-816.
11. Donato F, Tagger A, Gelatti U, Parrinello G, Boffetta P, Albertini A, Decarli A, Trevisi P, Ribero ML, Martelli C, Porru S, Nardi G. 2002. Alcohol and hepatocellular carcinoma: the effect of lifetime intake and hepatitis virus infections in men and women. Am J Epidemiol 155:323-331.
12. Anonymous. 1987. Overall evaluations of carcinogenicity: an updating of IARC Monographs volumes 1 to 42. IARC Monogr Eval Carcinog Risks Hum Suppl 7:1-440.
13. El-Serag HB, Hampel H, Javadi F. 2006. The association between diabetes and hepatocellular carcinoma: a systematic review of epidemiologic evidence. Clin Gastroenterol Hepatol 4:369-380.
14. Pikarsky E, Porat RM, Stein I, Abramovitch R, Amit S, Kasem S, Gutkovich-Pyest E, Urieli-Shoval S, Galun E, Ben-Neriah Y. 2004. NF-kappaB functions as a tumour promoter in inflammation-associated cancer. Nature 431:461-466.
15. Sakurai T, Maeda S, Chang L, Karin M. 2006. Loss of hepatic NF-kappa B activity enhances chemical hepatocarcinogenesis through sustained c-Jun N-terminal kinase 1 activation. Proc Natl Acad Sci U S A 103:10544-10551.
16. Maeda S, Kamata H, Luo JL, Leffert H, Karin M. 2005. IKKbeta couples hepatocyte death to cytokine-driven compensatory proliferation that promotes chemical hepatocarcinogenesis. Cell 121:977-990.
17. Luedde T, Beraza N, Kotsikoris V, van Loo G, Nenci A, De Vos R, Roskams T, Trautwein C, Pasparakis M. 2007. Deletion of NEMO/IKKgamma in liver

parenchymal cells causes steatohepatitis and hepatocellular carcinoma. Cancer Cell 11:119-132.
18. El-Serag HB, Marrero JA, Rudolph L, Reddy KR. 2008. Diagnosis and treatment of hepatocellular carcinoma. Gastroenterology 134:1752-1763.
19. Bruix J, Reig M, Sherman M. 2016. Evidence-based Diagnosis, Staging, and Treatment of Patients With Hepatocellular Carcinoma. Gastroenterology doi:10.1053/j.gastro.2015.12.041.
20. Bolondi L, Sofia S, Siringo S, Gaiani S, Casali A, Zironi G, Piscaglia F, Gramantieri L, Zanetti M, Sherman M. 2001. Surveillance programme of cirrhotic patients for early diagnosis and treatment of hepatocellular carcinoma: a cost effectiveness analysis. Gut 48:251-259.
21. Collier J, Sherman M. 1998. Screening for hepatocellular carcinoma. Hepatology 27:273-278.
22. Kim CK, Lim JH, Lee WJ. 2001. Detection of hepatocellular carcinomas and dysplastic nodules in cirrhotic liver: accuracy of ultrasonography in transplant patients. J Ultrasound Med 20:99-104.
23. Choi D, Kim SH, Lim JH, Cho JM, Lee WJ, Lee SJ, Lim HK. 2001. Detection of hepatocellular carcinoma: combined T2-weighted and dynamic gadolinium-enhanced MRI versus combined CT during arterial portography and CT hepatic arteriography. J Comput Assist Tomogr 25:777-785.
24. de Ledinghen V, Laharie D, Lecesne R, Le Bail B, Winnock M, Bernard PH, Saric J, Couzigou P, Balabaud C, Bioulac-Sage P, Drouillard J. 2002. Detection of nodules in liver cirrhosis: spiral computed tomography or magnetic resonance imaging? A prospective study of 88 nodules in 34 patients. Eur J Gastroenterol Hepatol 14:159-165.
25. Libbrecht L, Bielen D, Verslype C, Vanbeckevoort D, Pirenne J, Nevens F, Desmet V, Roskams T. 2002. Focal lesions in cirrhotic explant livers: pathological evaluation and accuracy of pretransplantation imaging examinations. Liver Transpl 8:749-761.
26. Rode A, Bancel B, Douek P, Chevallier M, Vilgrain V, Picaud G, Henry L, Berger F, Bizollon T, Gaudin JL, Ducerf C. 2001. Small nodule detection in cirrhotic livers: evaluation with US, spiral CT, and MRI and correlation with pathologic examination of explanted liver. J Comput Assist Tomogr 25:327-336.
27. Lee YJ, Lee JM, Lee JS, Lee HY, Park BH, Kim YH, Han JK, Choi BI. 2015. Hepatocellular carcinoma: diagnostic performance of multidetector CT and MR imaging-a systematic review and meta-analysis. Radiology 275:97-109.
28. Rasool M, Rashid S, Arooj M, Ansari SA, Khan KM, Malik A, Naseer MI, Zahid S, Manan A, Asif M, Razzaq Z, Ashraf S, Qazi MH, Iqbal Z, Gan SH, Kamal MA, Sheikh IA. 2014. New possibilities in hepatocellular carcinoma treatment. Anticancer Res 34:1563-1571.
29. Davila JA, El-Serag HB. 2006. Racial differences in survival of hepatocellular carcinoma in the United States: a population-based study. Clin Gastroenterol Hepatol 4:104-110; quiz 104-105.
30. Heindryckx F, Colle I, Van Vlierberghe H. 2009. Experimental mouse models for hepatocellular carcinoma research. Int J Exp Pathol 90:367-386.
31. Frese KK, Tuveson DA. 2007. Maximizing mouse cancer models. Nat Rev Cancer 7:645-658.
32. Verna L, Whysner J, Williams GM. 1996. N-nitrosodiethylamine mechanistic data and risk assessment: bioactivation, DNA-adduct formation, mutagenicity, and tumor initiation. Pharmacol Ther 71:57-81.

33. Qi Y, Chen X, Chan CY, Li D, Yuan C, Yu F, Lin MC, Yew DT, Kung HF, Lai L. 2008. Two-dimensional differential gel electrophoresis/analysis of diethylnitrosamine induced rat hepatocellular carcinoma. Int J Cancer 122:2682-2688.
34. Kawanishi S, Hiraku Y, Murata M, Oikawa S. 2002. The role of metals in site-specific DNA damage with reference to carcinogenesis. Free Radic Biol Med 32:822-832.
35. Valko M, Rhodes CJ, Moncol J, Izakovic M, Mazur M. 2006. Free radicals, metals and antioxidants in oxidative stress-induced cancer. Chem Biol Interact 160:1-40.
36. Rao KV, Vesselinovitch SD. 1973. Age- and sex-associated diethylnitrosamine dealkylation activity of the mouse liver and hepatocarcinogenesis. Cancer Res 33:1625-1627.
37. Vesselinovitch SD, Mihailovich N. 1983. Kinetics of diethylnitrosamine hepatocarcinogenesis in the infant mouse. Cancer Res 43:4253-4259.
38. Nakatani T, Roy G, Fujimoto N, Asahara T, Ito A. 2001. Sex hormone dependency of diethylnitrosamine-induced liver tumors in mice and chemoprevention by leuprorelin. Jpn J Cancer Res 92:249-256.
39. Lee JS, Chu IS, Mikaelyan A, Calvisi DF, Heo J, Reddy JK, Thorgeirsson SS. 2004. Application of comparative functional genomics to identify best-fit mouse models to study human cancer. Nat Genet 36:1306-1311.
40. Burdge GC, Calder PC. 2005. Conversion of alpha-linolenic acid to longer-chain polyunsaturated fatty acids in human adults. Reprod Nutr Dev 45:581-597.
41. Arterburn LM, Hall EB, Oken H. 2006. Distribution, interconversion, and dose response of n-3 fatty acids in humans. Am J Clin Nutr 83:1467S-1476S.
42. Simopoulos AP. 2002. The importance of the ratio of omega-6/omega-3 essential fatty acids. Biomed Pharmacother 56:365-379.
43. Simopoulos AP. 2006. Evolutionary aspects of diet, the omega-6/omega-3 ratio and genetic variation: nutritional implications for chronic diseases. Biomed Pharmacother 60:502-507.
44. Hibbeln JR, Nieminen LR, Blasbalg TL, Riggs JA, Lands WE. 2006. Healthy intakes of n-3 and n-6 fatty acids: estimations considering worldwide diversity. Am J Clin Nutr 83:1483S-1493S.
45. Weylandt KH, Kang JX. 2005. Rethinking lipid mediators. Lancet 366:618-620.
46. Pollard T, Earnshaw W. 2007. Cell Biology, 2 ed. Spektrum Akademischer Verlag, Berlin Heidelberg.
47. Nelson D, Cox M. 2008. Lehninger Principles of Biochemistry, 5 ed. W. H. Freeman and Company, New York.
48. Spector AA, Fang X, Snyder GD, Weintraub NL. 2004. Epoxyeicosatrienoic acids (EETs): metabolism and biochemical function. Prog Lipid Res 43:55-90.
49. Serhan CN. 2007. Resolution phase of inflammation: novel endogenous anti-inflammatory and proresolving lipid mediators and pathways. Annu Rev Immunol 25:101-137.
50. Serhan CN, Clish CB, Brannon J, Colgan SP, Chiang N, Gronert K. 2000. Novel functional sets of lipid-derived mediators with antiinflammatory actions generated from omega-3 fatty acids via cyclooxygenase 2-nonsteroidal antiinflammatory drugs and transcellular processing. J Exp Med 192:1197-1204.
51. Serhan CN, Hong S, Gronert K, Colgan SP, Devchand PR, Mirick G, Moussignac RL. 2002. Resolvins: a family of bioactive products of omega-3 fatty acid

transformation circuits initiated by aspirin treatment that counter proinflammation signals. J Exp Med 196:1025-1037.
52. Hong S, Gronert K, Devchand PR, Moussignac RL, Serhan CN. 2003. Novel docosatrienes and 17S-resolvins generated from docosahexaenoic acid in murine brain, human blood, and glial cells. Autacoids in anti-inflammation. J Biol Chem 278:14677-14687.
53. Arita M, Bianchini F, Aliberti J, Sher A, Chiang N, Hong S, Yang R, Petasis NA, Serhan CN. 2005. Stereochemical assignment, antiinflammatory properties, and receptor for the omega-3 lipid mediator resolvin E1. J Exp Med 201:713-722.
54. Arita M, Yoshida M, Hong S, Tjonahen E, Glickman JN, Petasis NA, Blumberg RS, Serhan CN. 2005. Resolvin E1, an endogenous lipid mediator derived from omega-3 eicosapentaenoic acid, protects against 2,4,6-trinitrobenzene sulfonic acid-induced colitis. Proc Natl Acad Sci U S A 102:7671-7676.
55. Marcheselli VL, Hong S, Lukiw WJ, Tian XH, Gronert K, Musto A, Hardy M, Gimenez JM, Chiang N, Serhan CN, Bazan NG. 2003. Novel docosanoids inhibit brain ischemia-reperfusion-mediated leukocyte infiltration and pro-inflammatory gene expression. J Biol Chem 278:43807-43817.
56. Gronert K, Maheshwari N, Khan N, Hassan IR, Dunn M, Laniado Schwartzman M. 2005. A role for the mouse 12/15-lipoxygenase pathway in promoting epithelial wound healing and host defense. J Biol Chem 280:15267-15278.
57. Ariel A, Li PL, Wang W, Tang WX, Fredman G, Hong S, Gotlinger KH, Serhan CN. 2005. The docosatriene protectin D1 is produced by TH2 skewing and promotes human T cell apoptosis via lipid raft clustering. J Biol Chem 280:43079-43086.
58. Serhan CN, Gotlinger K, Hong S, Lu Y, Siegelman J, Baer T, Yang R, Colgan SP, Petasis NA. 2006. Anti-inflammatory actions of neuroprotectin D1/protectin D1 and its natural stereoisomers: assignments of dihydroxy-containing docosatrienes. J Immunol 176:1848-1859.
59. Gonzalez-Periz A, Planaguma A, Gronert K, Miquel R, Lopez-Parra M, Titos E, Horrillo R, Ferre N, Deulofeu R, Arroyo V, Rodes J, Claria J. 2006. Docosahexaenoic acid (DHA) blunts liver injury by conversion to protective lipid mediators: protectin D1 and 17S-hydroxy-DHA. FASEB J 20:2537-2539.
60. Calder PC. 2002. Dietary modification of inflammation with lipids. Proc Nutr Soc 61:345-358.
61. Schmocker C, Weylandt KH, Kahlke L, Wang J, Lobeck H, Tiegs G, Berg T, Kang JX. 2007. Omega-3 fatty acids alleviate chemically induced acute hepatitis by suppression of cytokines. Hepatology 45:864-869.
62. Hudert CA, Weylandt KH, Lu Y, Wang J, Hong S, Dignass A, Serhan CN, Kang JX. 2006. Transgenic mice rich in endogenous omega-3 fatty acids are protected from colitis. Proc Natl Acad Sci U S A 103:11276-11281.
63. Arita M, Clish CB, Serhan CN. 2005. The contributions of aspirin and microbial oxygenase to the biosynthesis of anti-inflammatory resolvins: novel oxygenase products from omega-3 polyunsaturated fatty acids. Biochem Biophys Res Commun 338:149-157.
64. Puri P, Baillie RA, Wiest MM, Mirshahi F, Choudhury J, Cheung O, Sargeant C, Contos MJ, Sanyal AJ. 2007. A lipidomic analysis of nonalcoholic fatty liver disease. Hepatology 46:1081-1090.
65. Puri P, Wiest MM, Cheung O, Mirshahi F, Sargeant C, Min HK, Contos MJ, Sterling RK, Fuchs M, Zhou H, Watkins SM, Sanyal AJ. 2009. The plasma lipidomic signature of nonalcoholic steatohepatitis. Hepatology 50:1827-1838.

66. Kang JX. 2007. Fat-1 transgenic mice: a new model for omega-3 research. Prostaglandins Leukot Essent Fatty Acids 77:263-267.
67. Kang JX, Wang J, Wu L, Kang ZB. 2004. Transgenic mice: fat-1 mice convert n-6 to n-3 fatty acids. Nature 427:504.
68. Sakurai T, Maeda S, Chang L, Karin M. 2006. Inaugural Article: Loss of hepatic NF-{kappa}B activity enhances chemical hepatocarcinogenesis through sustained c-Jun N-terminal kinase 1 activation. Proc Natl Acad Sci U S A 103:10544-10551.
69. Seki E, Brenner DA. 2007. The role of NF-kappaB in hepatocarcinogenesis: promoter or suppressor? J Hepatol 47:307-309.
70. Karin M. 2006. NF-kappaB and cancer: mechanisms and targets. Mol Carcinog 45:355-361.
71. Greten FR, Eckmann L, Greten TF, Park JM, Li ZW, Egan LJ, Kagnoff MF, Karin M. 2004. IKKbeta links inflammation and tumorigenesis in a mouse model of colitis-associated cancer. Cell 118:285-296.
72. Fausto N. 1999. Mouse liver tumorigenesis: models, mechanisms, and relevance to human disease. Semin Liver Dis 19:243-252.
73. Endres S, Ghorbani R, Kelley VE, Georgilis K, Lonnemann G, van der Meer JW, Cannon JG, Rogers TS, Klempner MS, Weber PC, et al. 1989. The effect of dietary supplementation with n-3 polyunsaturated fatty acids on the synthesis of interleukin-1 and tumor necrosis factor by mononuclear cells. N Engl J Med 320:265-271.
74. Griffitts J, Saunders D, Tesiram YA, Reid GE, Salih A, Liu S, Lydic TA, Busik JV, Kang JX, Towner RA. 2010. Non-mammalian fat-1 gene prevents neoplasia when introduced to a mouse hepatocarcinogenesis model: Omega-3 fatty acids prevent liver neoplasia. Biochim Biophys Acta 1801:1133-1144.
75. Lim K, Han C, Dai Y, Shen M, Wu T. 2009. Omega-3 polyunsaturated fatty acids inhibit hepatocellular carcinoma cell growth through blocking beta-catenin and cyclooxygenase-2. Mol Cancer Ther 8:3046-3055.
76. Kang JX, Wang J. 2005. A simplified method for analysis of polyunsaturated fatty acids. BMC Biochem 6:5.
77. Sarma DS, Rao PM, Rajalakshmi S. 1986. Liver tumour promotion by chemicals: models and mechanisms. Cancer Surv 5:781-798.
78. Naugler WE, Sakurai T, Kim S, Maeda S, Kim K, Elsharkawy AM, Karin M. 2007. Gender disparity in liver cancer due to sex differences in MyD88-dependent IL-6 production. Science 317:121-124.
79. Reitman S, Frankel S. 1957. A colorimetric method for the determination of serum glutamic oxalacetic and glutamic pyruvic transaminases. Am J Clin Pathol 28:56-63.
80. Bradford MM. 1976. A rapid and sensitive method for the quantitation of microgram quantities of protein utilizing the principle of protein-dye binding. Anal Biochem 72:248-254.
81. Kang JX, Man SF, Brown NE, Labrecque PA, Garg ML, Clandinin MT. 1992. Essential fatty acid metabolism in cultured human airway epithelial cells. Biochim Biophys Acta 1128:267-274.
82. Rivera J, Ward N, Hodgson J, Puddey IB, Falck JR, Croft KD. 2004. Measurement of 20-hydroxyeicosatetraenoic acid in human urine by gas chromatography-mass spectrometry. Clin Chem 50:224-226.
83. Gravaghi C, La Perle KM, Ogrodwski P, Kang JX, Quimby F, Lipkin M, Lamprecht SA. 2011. Cox-2 expression, PGE(2) and cytokines production are

inhibited by endogenously synthesized n-3 PUFAs in inflamed colon of fat-1 mice. J Nutr Biochem 22:360-365.
84. Hardman WE. 2004. (n-3) fatty acids and cancer therapy. J Nutr 134:3427S-3430S.
85. Larsson SC, Kumlin M, Ingelman-Sundberg M, Wolk A. 2004. Dietary long-chain n-3 fatty acids for the prevention of cancer: a review of potential mechanisms. Am J Clin Nutr 79:935-945.
86. Jelinska M, Tokarz A, Oledzka R, Czorniuk-Sliwa A. 2003. Effects of dietary linseed, evening primrose or fish oils on fatty acid and prostaglandin E2 contents in the rat livers and 7,12-dimethylbenz[a]anthracene-induced tumours. Biochim Biophys Acta 1637:193-199.
87. Kim Y, Ji SK, Choi H. 2000. Modulation of liver microsomal monooxygenase system by dietary n-6/n-3 ratios in rat hepatocarcinogenesis. Nutr Cancer 37:65-72.
88. Lii CK, Ou CC, Liu KL, Liu JY, Lin WL, Chen HW. 2000. Suppression of altered hepatic foci development by a high fish oil diet compared with a high corn oil diet in rats. Nutr Cancer 38:50-59.
89. He L, Tian DA, Li PY, He XX. 2015. Mouse models of liver cancer: Progress and recommendations. Oncotarget 6:23306-23322.
90. Simopoulos AP. 2011. Importance of the omega-6/omega-3 balance in health and disease: evolutionary aspects of diet. World Rev Nutr Diet 102:10-21.
91. Mazzaferro V, Llovet JM, Miceli R, Bhoori S, Schiavo M, Mariani L, Camerini T, Roayaie S, Schwartz ME, Grazi GL, Adam R, Neuhaus P, Salizzoni M, Bruix J, Forner A, De Carlis L, Cillo U, Burroughs AK, Troisi R, Rossi M, Gerunda GE, Lerut J, Belghiti J, Boin I, Gugenheim J, Rochling F, Van Hoek B, Majno P. 2009. Predicting survival after liver transplantation in patients with hepatocellular carcinoma beyond the Milan criteria: a retrospective, exploratory analysis. Lancet Oncol 10:35-43.
92. Bogaerts E, Heindryckx F, Devisscher L, Paridaens A, Vandewynckel YP, Van den Bussche A, Verhelst X, Libbrecht L, van Grunsven LA, Geerts A, Van Vlierberghe H. 2015. Time-dependent effect of hypoxia on tumor progression and liver progenitor cell markers in primary liver tumors. PLoS One 10:e0119555.
93. Lu XF, Zhou YJ, Zhang L, Ji HJ, Li L, Shi YJ, Bu H. 2015. Loss of Dicer1 impairs hepatocyte survival and leads to chronic inflammation and progenitor cell activation. World J Gastroenterol 21:6591-6603.
94. Schmocker C, Weylandt KH, Kahlke L, Wang J, Lobeck H, Tiegs G, Berg T, Kang JX. 2007. Omega-3 fatty acids alleviate chemically induced acute hepatitis by suppression of cytokines. Hepatology 45:864-869.
95. Wu T. 2006. Cyclooxygenase-2 in hepatocellular carcinoma. Cancer Treat Rev 32:28-44.
96. Agarwal S, Reddy GV, Reddanna P. 2009. Eicosanoids in inflammation and cancer: the role of COX-2. Expert Rev Clin Immunol 5:145-165.
97. Weylandt KH, Chiu CY, Gomolka B, Waechter SF, Wiedenmann B. 2012. Omega-3 fatty acids and their lipid mediators: towards an understanding of resolvin and protectin formation. Prostaglandins Other Lipid Mediat 97:73-82.
98. Chiu CY, Gomolka B, Dierkes C, Huang NR, Schroeder M, Purschke M, Manstein D, Dangi B, Weylandt KH. 2012. Omega-6 docosapentaenoic acid-derived resolvins and 17-hydroxydocosahexaenoic acid modulate macrophage function and alleviate experimental colitis. Inflamm Res 61:967-976.

99. Weylandt KH, Nadolny A, Kahlke L, Kohnke T, Schmocker C, Wang J, Lauwers GY, Glickman JN, Kang JX. 2008. Reduction of inflammation and chronic tissue damage by omega-3 fatty acids in fat-1 transgenic mice with pancreatitis. Biochim Biophys Acta 1782:634-641.
100. Sun XF, Zhang H. 2007. NFKB and NFKBI polymorphisms in relation to susceptibility of tumour and other diseases. Histol Histopathol 22:1387-1398.
101. Nowak J, Weylandt KH, Habbel P, Wang J, Dignass A, Glickman JN, Kang JX. 2007. Colitis-associated colon tumorigenesis is suppressed in transgenic mice rich in endogenous n-3 fatty acids. Carcinogenesis 28:1991-1995.
102. Kim EH, Bae JS, Hahm KB, Cha JY. 2012. Endogenously synthesized n-3 polyunsaturated fatty acids in fat-1 mice ameliorate high-fat diet-induced non-alcoholic fatty liver disease. Biochem Pharmacol 84:1359-1365.
103. Bilal S, Haworth O, Wu L, Weylandt KH, Levy BD, Kang JX. 2011. Fat-1 transgenic mice with elevated omega-3 fatty acids are protected from allergic airway responses. Biochim Biophys Acta 1812:1164-1169.
104. Jiang JG, Chen CL, Card JW, Yang S, Chen JX, Fu XN, Ning YG, Xiao X, Zeldin DC, Wang DW. 2005. Cytochrome P450 2J2 promotes the neoplastic phenotype of carcinoma cells and is up-regulated in human tumors. Cancer Res 65:4707-4715.
105. Jiang JG, Ning YG, Chen C, Ma D, Liu ZJ, Yang S, Zhou J, Xiao X, Zhang XA, Edin ML, Card JW, Wang J, Zeldin DC, Wang DW. 2007. Cytochrome p450 epoxygenase promotes human cancer metastasis. Cancer Res 67:6665-6674.
106. Webler AC, Michaelis UR, Popp R, Barbosa-Sicard E, Murugan A, Falck JR, Fisslthaler B, Fleming I. 2008. Epoxyeicosatrienoic acids are part of the VEGF-activated signaling cascade leading to angiogenesis. Am J Physiol Cell Physiol 295:C1292-1301.
107. Weylandt KH, Krause LF, Gomolka B, Chiu CY, Bilal S, Nadolny A, Waechter SF, Fischer A, Rothe M, Kang JX. 2011. Suppressed liver tumorigenesis in fat-1 mice with elevated omega-3 fatty acids is associated with increased omega-3 derived lipid mediators and reduced TNF-alpha. Carcinogenesis 32:897-903.
108. Endo J, Sano M, Isobe Y, Fukuda K, Kang JX, Arai H, Arita M. 2014. 18-HEPE, an n-3 fatty acid metabolite released by macrophages, prevents pressure overload-induced maladaptive cardiac remodeling. J Exp Med 211:1673-1687.
109. Serhan CN, Chiang N. 2008. Endogenous pro-resolving and anti-inflammatory lipid mediators: a new pharmacologic genus. Br J Pharmacol 153 Suppl 1:S200-215.
110. Gleissman H, Yang R, Martinod K, Lindskog M, Serhan CN, Johnsen JI, Kogner P. 2010. Docosahexaenoic acid metabolome in neural tumors: identification of cytotoxic intermediates. FASEB J 24:906-915.

8 Affirmation / Eidesstattliche Versicherung

„Ich, Lena Olgun, versichere an Eides statt durch meine eigenhändige Unterschrift, dass ich die vorgelegte Dissertation mit dem Thema: „The effect of omega-3 fatty acids on hepatocellular carcinoma in a transgenic mouse model“ selbstständig und ohne nicht offengelegte Hilfe Dritter verfasst und keine anderen als die angegebenen Quellen und Hilfsmittel genutzt habe.
Alle Stellen, die wörtlich oder dem Sinne nach auf Publikationen oder Vorträgen anderer Autoren beruhen, sind als solche in korrekter Zitierung (siehe „Uniform Requirements for Manuscripts (URM)“ des ICMJE - www.icmje.org) kenntlich gemacht. Die Abschnitte zu Methodik (insbesondere praktische Arbeiten, Laborbestimmungen, statistische Aufarbeitung) und Resultaten (insbesondere Abbildungen, Graphiken und Tabellen) entsprechen den URM (s.o.) und werden von mir verantwortet.
Meine Anteile an etwaigen Publikationen zu dieser Dissertation entsprechen denen, die in der untenstehenden gemeinsamen Erklärung mit dem Betreuer angegeben sind. Sämtliche Publikationen, die aus dieser Dissertation hervorgegangen sind und bei denen ich Autor bin, entsprechen den URM und werden von mir verantwortet.

Die Bedeutung dieser eidesstattlichen Versicherung und die strafrechtlichen Folgen einer unwahren eidesstattlichen Versicherung (§156,161 des Strafgesetzbuches) sind mir bekannt und bewusst.“

Datum Unterschrift

Anteilserklärung an etwaigen erfolgten Publikationen

Lena Friederike Olgun (geb. Krause) hatte folgenden Anteil an der folgenden Publikation:

Weylandt KH*, **Krause LF***, Gomolka B, Chiu CY, Bilal S, Nadolny A, Waechter SF, Fischer A, Rothe M, Kang JX (* equally contributed). *Suppressed liver tumorigenesis in fat-1 mice with elevated omega-3 fatty acids is associated with increased omega-3 derived lipid mediators and reduced TNF-α.* Carcinogenesis. 2011 Jun;32(6):897-903.

Beitrag im Einzelnen:
Lena Olgun (geb. Krause) ist geteilte Erstautorin gemeinsam mit Karsten Weylandt für diese Publikation. Lena Olgun hat folgende Experimente selbstständig durchgeführt und ausgewertet: Auszählung und Messen der Tumore mittels Stereomikroskopie, Entnahme und Präparation der Organe für histologische Untersuchungen, Anfertigung der Hämatoxylin-Eosin-Färbung für die weitere Analyse durch den Pathologen Dr. Jonathan Glickman, Durchführung und Auswertung der immunhistochemischen Versuche, Durchführung der Gas-Chromatographie zur Identifizierung der mehrfach ungesättigten Fettsäuren in Lebern der Wildtyp- und fat-1 Mäuse, Durchführung der Serumanalysen der Transaminasen ALT und AST, und des TNF-α ELISAs. Desweiteren erfolgte die statistische Auswertung dieser Ergebnisse durch Lena Olgun in Zusammenarbeit mit Karsten Weylandt.

Unterschrift, Datum und Stempel des betreuenden Hochschullehrers

Unterschrift der Doktorandin

9 Curriculum Vitae / Lebenslauf

Mein Lebenslauf wird aus datenschutzrechtlichen Gründen in der elektronischen Version meiner Arbeit nicht veröffentlicht.

10 List of Publications / Publikationsliste

Weylandt KH*, **Krause LF***, Gomolka B, Chiu CY, Bilal S, Nadolny A, Waechter SF, Fischer A, Rothe M, Kang JX (* equally contributed). *Suppressed liver tumorigenesis in fat-1 mice with elevated omega-3 fatty acids is associated with increased omega-3 derived lipid mediators and reduced TNF-α.* Carcinogenesis. 2011 Jun;32(6):897-903.

11 Acknowledgments / Danksagung

Sehr herzlich bedanke ich mich bei PD Dr. Dr. med. Karsten H. Weylandt für die Überlassung des interessanten Themas, seine intensive wissenschaftliche Betreuung, seine vielen zielführenden Ideen und engagierten Diskussionen sowie die nette Zusammenarbeit.

Den Mitarbeitern des Laboratory for Lipid Medicine and Technology des Massachusetts General Hospital danke ich für die enge Zusammenarbeit und Hilfe. Insbesondere möchte ich mich bei Dr. Jing X. Kang, Dr. Jingdong Wang und Dr. Chengwei He für die freundliche Aufnahme und stete Unterstützung in Boston bedanken. Ich danke Dr. rer. medic. Beate Gomolka und Dr. rer. nat. Michael Rothe für die Zusammenarbeit bei der Analyse der Lipidmediatoren, Dr. Jonathan Glickman für die histopathologische Auswertung und Dr. Xiangzhi Zhou und Dr. Yanping Sun für die Hilfe bei der Etablierung und Durchführung der MRT-Messungen.

Ganz besonderer Dank gilt meinen Laborpartnern Dr. med. Simon Wächter, Dr. med. Thomas Köhnke und Anja Nadolny für die kollegiale und freundschaftliche Zusammenarbeit.